# 10

# Nonlocal Homogenization Theory of Structured Materials




Mário G. Silveirinha
*University of Coimbra*


## 10.1 Introduction

The use of homogenization methods in characterizing the interaction of electromagnetic fields with matter has a long history. An interesting review of the pioneering works of Lorentz, Planck, Ewald, and Oseen is given in [1]. Lorentz was the first to recognize that to properly describe molecular optics it was necessary to incorporate atomic concepts into Maxwell's equations, and take into account the electric vibrations of the particles. He obtained a relation between the dielectric constant and the density of the material at optical frequencies, and established the foundations of macroscopic electromagnetism. During the last century, the theory was further developed by studies that clarified averaging procedures [2], and took into account the resonant interaction of electromagnetic radiation with dielectric crystals coupled via retarded dipole fields [3]. Classical molecular optics was also extended to optically active media and to spatially dispersive media [4,5].

In recent years, there has been a renewed interest in homogenization methods due to their application in the characterization of structured materials (metamaterials). These materials are formed by properly shaped dielectric or metallic inclusions designed to obtain a desired effective response of

the material. It has been demonstrated that metamaterials may enable anomalous phenomena, such as negative refraction [6], compression of waves through very narrow channels [7], or subwavelength imaging [8–11].

The simplest homogenization approach is based on the use of mixing formulas, such as the Clausius–Mossotti formula [12]. The Clausius–Mossotti formula requires the volume fraction of the inclusions to be small, in order that they can be accurately modeled as point dipoles. More general homogenization methods have been developed over the years [13–18], but their applications are usually restricted to the quasistatic limit or to very specific geometries, or are limited by some other factor.

A key property of novel metamaterials is that the wavelength of light is only moderately larger than the lattice constant $a$, typically 5–10 times. This contrasts markedly with propagation of radiation in matter where the ratio, $\lambda/a$, is several orders of magnitude larger than that value, even at optical frequencies. This property may impose some restrictions on the application of classical homogenization theories to artificial materials [19]. In particular, the role of spatial dispersion in microstructured materials has been underlined by recent works [20–28]. Spatially dispersive materials may have important applications, such as imaging with super-resolution [10] or the realization of impedance surfaces [29].

The objective of this chapter is to present the state of art of homogenization methods for spatially dispersive materials. First, in Section 10.2, we discuss the definitions of the macroscopic fields, averaging procedures, and constitutive relations in local media. In Section 10.3, the homogenization theory introduced in [30] is described. This theory enables the calculation of the nonlocal dielectric function, $\underline{\underline{\varepsilon}} = \underline{\underline{\varepsilon}}(\omega, \mathbf{k})$, of an arbitrary periodic, composite dielectric material. To illustrate the application of such a homogenization approach, in Section 10.4 the dielectric function of a crystal formed by electric dipoles is explicitly calculated. In Section 10.5, it is explained how the homogenization method can be numerically implemented using the method of moments (MoM). Then, in Section 10.6, the relation between the local effective parameters and the nonlocal dielectric function is discussed. Finally, in Section 10.7, the problem of additional boundary conditions in spatially dispersive media is studied. The time variation, $e^{j\omega t}$, is assumed in this chapter.

## 10.2 Macroscopic Electromagnetism and Constitutive Relations in Local Media

The homogenization theory is an attempt to describe the interaction of electromagnetic radiation with very complex systems formed by an extremely large number of atoms, or in case of microstructured materials, formed by many inclusions. Typically, homogenization concepts may be applied when the wavelength of radiation is much larger than the characteristic microscopic dimensions of the considered system. In such circumstances, it is possible to average out the microscopic fluctuations of the electromagnetic fields, and in this way obtain slowly varying and smooth macroscopic quantities, which can be used to characterize the long range variations (propagation) of the electromagnetic waves. A key concept in the homogenization theory is the notion of spatial averaging. The spatial average of a physical entity, $F(\mathbf{r})$, with respect to a test function, $f(\mathbf{r})$, is defined here as [2,12],

$$\langle F \rangle (\mathbf{r}) = \int F(\mathbf{r} - \mathbf{r}')\, f(\mathbf{r}')\, \mathrm{d}^3\mathbf{r}' \tag{10.1}$$

where

$\mathbf{r} = (x,\ y,\ z)$ is a generic point of space

$f(\mathbf{r})$ is a real-valued function, nonzero in some neighborhood of the origin, and such that its integral over all space is unity

It may also be imposed that $f$ is nonnegative, even though this is not strictly necessary. The support of $f(\mathbf{r})$ has a radial dimension $R$ much smaller than the wavelength, and $R$ is typically much larger than

the characteristic length of the microscopic domain (e.g., the lattice constant). The average field is, thus, given by the spatial convolution of the corresponding microscopic field with the test function. The main advantage of the considered averaging procedure is that it preserves the structure of the Maxwell equations, as detailed next.

To be specific, consider a material formed by nonmagnetic dielectric inclusions with relative permittivity $\varepsilon_r(\mathbf{r})$, and let $\mathbf{E}$ and $\mathbf{B}$ be the electric and induction fields in the material. These fields are designated here by microscopic fields, exploring the close analogy with the propagation of electromagnetic waves in matter. The fields $\mathbf{E}$ and $\mathbf{B}$ satisfy the frequency domain Maxwell equations,

$$\begin{aligned} \nabla \times \mathbf{E} &= -j\,\omega \mathbf{B} \\ \nabla \times \frac{\mathbf{B}}{\mu_0} &= \mathbf{J}_e + \varepsilon_0 \varepsilon_r j\omega\, \mathbf{E} \end{aligned} \tag{10.2}$$

where $\mathbf{J}_e$ is the applied electric current density (source of fields). The macroscopic fields, $\langle \mathbf{E} \rangle$ and $\langle \mathbf{B} \rangle$, are obtained by averaging the microscopic fields using the operator (Equation 10.1). The test function $f$ may be rather arbitrary, and does not need to be specified in detail. It can be easily verified that the space derivatives commute with the averaging operator defined by Equation 10.1 [2,12]. Hence, the macroscopic fields satisfy the following macroscopic equations:

$$\begin{aligned} \nabla \times \langle \mathbf{E} \rangle &= -j\omega \langle \mathbf{B} \rangle \\ \nabla \times \frac{\langle \mathbf{B} \rangle}{\mu_0} &= \langle \mathbf{J}_e \rangle + \langle \mathbf{J}_d \rangle + j\omega \varepsilon_0 \langle \mathbf{E} \rangle \end{aligned} \tag{10.3}$$

In the above, $\mathbf{J}_d = \varepsilon_0 (\varepsilon_r - 1)\, j\omega,\ \mathbf{E}$ is the induced microscopic current relative to the host medium, which is assumed vacuum without loss of generality. The space averaged applied current, $\langle \mathbf{J}_e \rangle$, and the space averaged microscopic current, $\langle \mathbf{J}_d \rangle$, are defined consistently with Equation 10.1. By comparing Equations 10.2 and 10.3, it is clear that the structure of Maxwell equations is, indeed, preserved by the averaging operator.

The classical theories of macroscopic electromagnetism are based on the decomposition of the averaged microscopic currents $\langle \mathbf{J}_d \rangle$ into dipolar and higher-order contributions [12,31],

$$\langle \mathbf{J}_d \rangle \approx j\omega \mathbf{P} + \nabla \times \mathbf{M} + \cdots \tag{10.4}$$

where

$\mathbf{P}$ is the polarization vector
$\mathbf{M}$ is the magnetization vector

The terms that are omitted involve spatial derivatives of the quadrupole density and other higher-order multipole moments. The classical definition of the (macroscopic) electric displacement vector $\mathbf{D}$ and of the (macroscopic) magnetic field $\mathbf{H}$ is motivated by the decomposition (Equation 10.4) of the average microscopic current into mean and eddy currents. As is well known, $\mathbf{D}$ and $\mathbf{H}$ are related to the fundamental macroscopic fields through the textbook formulas,

$$\begin{aligned} \mathbf{D} &= \varepsilon_0 \langle \mathbf{E} \rangle + \mathbf{P} \\ \mathbf{H} &= \frac{\langle \mathbf{B} \rangle}{\mu_0} - \mathbf{M} \end{aligned} \tag{10.5}$$

Thus, Equation 10.5 implicitly absorbs the effect of the microscopic currents into $\mathbf{D}$ and $\mathbf{H}$, and so the macroscopic Maxwell equations in the material have the same form as in vacuum, apart from the relation between $\langle \mathbf{E} \rangle$, $\mathbf{D}$, $\langle \mathbf{B} \rangle$, and $\mathbf{H}$. For linear materials, $\mathbf{P}$ and $\mathbf{M}$ may be written as a linear combination of $\langle \mathbf{E} \rangle$ and $\mathbf{H}$. Such materials form the general class of bianisotropic materials [32,33] and are characterized by the constitutive relations,

$$\mathbf{D} = \varepsilon_0 \underline{\varepsilon_r} \cdot \langle \mathbf{E} \rangle + \sqrt{\varepsilon_0 \mu_0}\, \underline{\boldsymbol{\xi}} \cdot \mathbf{H}$$
$$\langle \mathbf{B} \rangle = \sqrt{\varepsilon_0 \mu_0}\, \underline{\boldsymbol{\zeta}} \cdot \langle \mathbf{E} \rangle + \mu_0 \underline{\boldsymbol{\mu}_r} \cdot \mathbf{H} \tag{10.6}$$

where

$\underline{\varepsilon_r}(\omega)$ is the relative permittivity
$\underline{\boldsymbol{\mu}_r}(\omega)$ is the relative permeability
$\underline{\boldsymbol{\xi}}(\omega)$ and $\underline{\boldsymbol{\zeta}}(\omega)$ are (dimensionless) parameters that characterize the magnetoelectric coupling

When the structure has a center of inversion symmetry the terms $\underline{\boldsymbol{\xi}}$ and $\underline{\boldsymbol{\zeta}}$ vanish, and the material can be described using uniquely permittivity and permeability tensors.

It is stressed that the above phenomenological model is meaningful only when the approximation, $\langle \mathbf{J}_d \rangle \approx j\omega\mathbf{P} + \nabla \times \mathbf{M}$, holds, and the higher-order multipole moments are negligible. Moreover, it is implicit that the medium is local in the sense that $\mathbf{D}$ and $\mathbf{H}$ at a given point of space can be written exclusively in terms of $\langle \mathbf{E} \rangle$ and $\langle \mathbf{B} \rangle$ at the same point of space, as implied by Equation 10.6.* Otherwise the medium is characterized by spatial dispersion [4,31]. In ordinary natural materials, where the lattice constant, $a \sim 0.1\ nm$, is several orders of magnitude smaller than the wavelength of radiation, the enunciated conditions are typically verified, and thus, the model (Equation 10.6) usually describes adequately macroscopic electromagnetism. However, in common artificial materials the lattice constant is typically only marginally smaller than the wavelength of radiation, and so the nonlocal effects may not be negligible, and the approximation (Equation 10.4) may not be accurate. Moreover, the phenomenological model (Equation 10.6) may also be inadequate to characterize natural media at optical frequencies, because, as argued in [31], the "the magnetic permeability ceases to have physical meaning at relatively low frequencies." It is thus clear that more sophisticated homogenization methods and concepts are necessary to characterize novel materials. The objective of this chapter is to present a fresh overview of these methods.

## 10.3 Homogenization of Nonlocal Media

Spatial dispersion effects occur when the polarization and magnetization vectors at a given "point" of space cannot be related through local relations with the macroscopic fields $\langle \mathbf{E} \rangle$ and $\langle \mathbf{B} \rangle$. Nonlocal effects have been studied in crystal optics, plasma physics, and metal optics [4], and more recently in artificial materials [20–28].

The goal of this section is to describe homogenization methods in spatially dispersive media. Our analysis closely follows reference [30]. It is assumed that the artificial material is nonmagnetic and periodic, with generic geometry as in Figure 10.1. The medium is invariant to translations along the primitive vectors $\mathbf{a}_1$, $\mathbf{a}_2$, and $\mathbf{a}_3$. Hence, the permittivity of the inclusions satisfies $\varepsilon_r(\mathbf{r} + \mathbf{r_I}) = \varepsilon_r(\mathbf{r})$, where $\mathbf{r_I} = i_1\mathbf{a}_1 + i_2\mathbf{a}_2 + i_3\mathbf{a}_3$ is a lattice point and $\mathbf{I} = (i_1, i_2, i_3)$ is a generic multi-index of integers. The unit cell $\Omega$ of the periodic medium is $\Omega = \{\alpha_1\mathbf{a}_1 + \alpha_2\mathbf{a}_2 + \alpha_3\mathbf{a}_3 : |\alpha_i| \le 1/2\}$. The permittivity may be a complex number and depend on frequency. In addition, the unit cell may contain perfectly electric conducting (PEC) metallic surfaces, which are denoted by $\partial D$, as illustrated in Figure 10.1. The outward unit vector normal to $\partial D$ is $\hat{\mathbf{v}}$.

*Some authors consider that media with magnetoelectric activity are nonlocal, since such an effect may be regarded as a manifestation of the first-order spatial dispersion. Here, we follow a slightly different definition, and consider that when it is possible to relate the macroscopic fields through local relations in the space domain as in Equation 10.6, the medium is by definition local and linear.

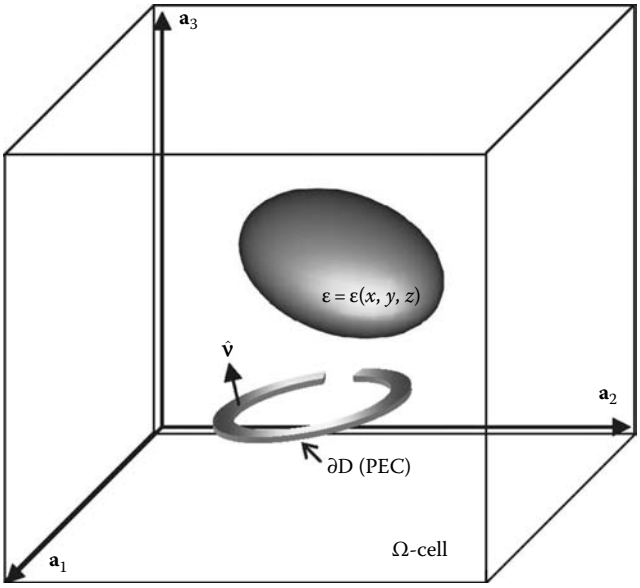


**FIGURE 10.1** Geometry of the unit cell of a generic metallic-dielectric periodic material with a dielectric inclusion and a PEC inclusion. (Reprinted from Silveirinha, M.G., *Phys. Rev. B*, 75, 115104, 2007. With permission.)

### 10.3.1 Constitutive Relations in Nonlocal Media

In presence of strong spatial dispersion, the introduction of the effective permeability tensor $\underline{\boldsymbol{\mu}}_{\mathbf{r}}$, as well as of $\underline{\boldsymbol{\xi}}$ and $\underline{\boldsymbol{\zeta}}$, is not meaningful [31]. The problem is that splitting the mean microscopic current as in Equation 10.4 is not advantageous, because **P** and **M** cannot be related with the average fields through local relations. Due to this reason, it is common to consider alternative phenomenological constitutive relations, in which all the terms resulting from the averaging of the microscopic currents are directly included into the definition of the electric displacement **D**, without introducing a magnetization vector. In this way, for a nonlocal medium we have the following definitions [4,31] (compare with Equation 10.5):

$$\begin{aligned} \mathbf{D}_{\mathrm{g}} &= \varepsilon_0 \langle \mathbf{E} \rangle + \mathbf{P}_{\mathrm{g}} \\ \mathbf{H}_{\mathrm{g}} &= \frac{\langle \mathbf{B} \rangle}{\mu_0} \end{aligned} \tag{10.7}$$

where, by definition, $\mathbf{P}_{\mathrm{g}} = \langle \mathbf{J}_{\mathrm{d}} \rangle / j\omega$. We introduced the subscript "g" to underline that the electric displacement and the magnetic field defined as in Equation 10.7 differ from the classical definition (Equation 10.5). In fact, as mentioned above, in this phenomenological model all the microscopic currents are included directly in the definition of the electric displacement. From Equation 10.4, it is evident that

$$\mathbf{P}_{\mathrm{g}} = \mathbf{P} + \nabla \times \mathbf{M} / j\omega + \cdots \tag{10.8}$$

Thus, $\mathbf{P}_{\mathrm{g}}$ is a generalized polarization vector that contains the effect of the dipolar moments, and in addition, the effect of all higher-order multipole moments.

The effective parameters corresponding to Equation 10.7 are completely different from the local effective parameters associated with Equation 10.6. In fact, $\mathbf{D}_{\mathrm{g}}$ cannot be related with the average field $\langle \mathbf{E} \rangle$ through a local relation, since, in general, the polarization $\mathbf{P}_{\mathrm{g}}$ at one point of space depends on the distribution of the macroscopic electric field in a neighborhood of the considered point. Instead,

for unbounded periodic linear materials, it is assumed that the macroscopic fields are related by a constitutive relation of the form [4,31]*

$$\mathbf{D}_g(\mathbf{r}) = \int \underline{\hat{\varepsilon}}\,(\omega, \mathbf{r} - \mathbf{r}') \cdot \langle \mathbf{E}(\mathbf{r}') \rangle \, d^3\mathbf{r}' \tag{10.9}$$

where $\underline{\hat{\varepsilon}}$ is the dielectric function of the material in the space domain. This constitutive relation establishes that the electric displacement is related to the macroscopic electric field through a space convolution. The nonlocal character of the material is clear from such a formula.

The relation between the macroscopic fields is comparatively simpler in the Fourier transform **k**-domain. The Fourier transform of the macroscopic electric field is, by definition,

$$\langle \tilde{\mathbf{E}} \rangle (\mathbf{k}) = \int \langle \mathbf{E}(\mathbf{r}) \rangle \, e^{j\mathbf{k}\cdot\mathbf{r}} d^3\mathbf{r} \tag{10.10}$$

where

"~" denotes Fourier transformation

$\mathbf{k} = (k_x, k_y, k_z)$ is the wave vector

From Equations 10.7 and 10.9, it is clear that in the spectral domain the following constitutive relations hold:

$$\begin{aligned} \tilde{\mathbf{D}}_g &\equiv \varepsilon_0 \langle \tilde{\mathbf{E}} \rangle + \tilde{\mathbf{P}}_g = \underline{\varepsilon}\,(\omega, \mathbf{k}) \cdot \langle \tilde{\mathbf{E}} \rangle \\ \tilde{\mathbf{H}}_g &= \frac{\langle \tilde{\mathbf{B}} \rangle}{\mu_0} \end{aligned} \tag{10.11}$$

where $\underline{\varepsilon}\,(\omega, \mathbf{k})$ is the dielectric function of the material, which is given by the Fourier transform of $\underline{\hat{\varepsilon}}$. The homogenized unbounded material is completely characterized by the dielectric function. When using the constitutive relations (Equation 10.7) it is not necessary to introduce a magnetic permeability tensor: all the physics is described by $\underline{\varepsilon}\,(\omega, \mathbf{k})$, including the effect of high order multipoles.

The parameters ω and **k** in the argument of the dielectric function are independent variables. This property should be obvious from the definition of $\underline{\varepsilon}$ [4]. Sometimes this may be a source of confusion, because for plane wave propagation, and in the absence of external sources, the wave vector becomes a function of frequency, $\mathbf{k} = \mathbf{k}(\omega)$. However, the key point is that the dielectric function is defined in its most general form even for ω and **k** that are not associated with plane wave normal modes. Indeed, as it is discussed in Section 10.3.3, to calculate the dielectric function the material must be excited by an external source. This makes possible the generation of microscopic fields associated with any independent values of ω and **k**.

## 10.3.2 Fields with Floquet Variation

Electromagnetic fields with Floquet periodicity are of special importance in the characterization of periodic media. For example, the electromagnetic properties of dielectric crystals are completely determined by the "band structure" of their Floquet eigenmodes. Thus, it is not surprising if the dielectric function of a structured material is closely related to the Floquet fields. To establish this connection in what follows, the macroscopic properties of electromagnetic fields with the Floquet

*For spatially inhomogeneous bodies, which ultimately is the case of all crystals, the dielectric function cannot be written as a function of $\mathbf{r} - \mathbf{r}'$, and is of the more general form $\underline{\hat{\varepsilon}}\,(\omega, \mathbf{r}, \mathbf{r}')$ [4, p. 87].

property are characterized. It will be shown that under suitable conditions the macroscopic fields may be identified with the amplitudes of the zero-order Floquet harmonics associated with the microscopic fields.

It is assumed that the electric field $\mathbf{E}$ is such that $\mathbf{E}(\mathbf{r})\, e^{j\mathbf{k}\cdot\mathbf{r}}$ is periodic, where $\mathbf{k}$ is the imposed wave vector. The microscopic induction field $\mathbf{B}$ and the applied current $\mathbf{J}_e$ have a similar property. Notice that $(\mathbf{E}, \mathbf{B})$ are not necessarily associated with an electromagnetic mode of the periodic material, because the applied current does not have to be zero.

In order to characterize the macroscopic fields in the spectral domain, the electric field is expanded into a Fourier series,

$$\begin{aligned} \mathbf{E}(\mathbf{r}) &= \sum_{\mathbf{J}} \mathbf{E}_{\mathbf{J}}\, e^{-j\mathbf{k}_{\mathbf{J}}\cdot\mathbf{r}}, \quad \mathbf{k}_{\mathbf{J}} = \mathbf{k} + \mathbf{k}_{\mathbf{J}}^{0} \\ \mathbf{E}_{\mathbf{J}} &= \frac{1}{V_{\text{cell}}} \int_{\Omega} \mathbf{E}(\mathbf{r})\, e^{j\mathbf{k}_{\mathbf{J}}\cdot\mathbf{r}} \mathrm{d}^3\mathbf{r} \end{aligned} \tag{10.12}$$

where

$V_{\text{cell}} = |\mathbf{a}_1 \cdot (\mathbf{a}_2 \times \mathbf{a}_3)|$ is the volume of the unit cell
$\mathbf{J} = (j_1, j_2, j_3)$ is a multi-index of integers
$\mathbf{k}_{\mathbf{J}}^{0} = j_1\mathbf{b}_1 + j_2\mathbf{b}_2 + j_3\mathbf{b}_3$
$\mathbf{E}_{\mathbf{J}}$ is the coefficient of the $\mathbf{J}$th harmonic

The reciprocal lattice primitive vectors, $\mathbf{b}_n$, are implicitly defined by the relations, $\mathbf{a}_m \cdot \mathbf{b}_n = 2\pi\delta_{m,n}$, $m, n = 1, 2, 3$.

From the definition of the averaging operator (Equation 10.1), it is clear that $\langle\tilde{\mathbf{E}}\rangle(\mathbf{k}') = \tilde{\mathbf{E}}(\mathbf{k}')\, \tilde{f}(\mathbf{k}')$, where $\tilde{\mathbf{E}}$ is the Fourier transform of the microscopic field and $\tilde{f}$ is the Fourier transform of the test function. Hence, using Equation 10.12, it is found that in the spectral domain

$$\langle\tilde{\mathbf{E}}\rangle(\mathbf{k}') = (2\pi)^3 \sum_{\mathbf{J}} \mathbf{E}_{\mathbf{J}} \tilde{f}(\mathbf{k}_{\mathbf{J}})\, \delta(\mathbf{k}' - \mathbf{k}_{\mathbf{J}}) \tag{10.13}$$

Thus, the macroscopic electric field in the spectral domain consists of a superimposition of Dirac $\delta$-function impulses centered at points of the form, $\mathbf{k}' = \mathbf{k}_{\mathbf{J}}$. The amplitudes of the impulses depend on the Fourier series coefficients of the microscopic field, as well as on the considered test function.

At this point it is convenient to analyze the properties of the test function $f$ with more detail. Since $f$ is normalized to unity, i.e., its integral over all space is unity, it follows that $\tilde{f}(\mathbf{0}) = 1$. In order to average out the microscopic fluctuations of the fields, it is sufficient that the support of $f$ in the space domain contains the unit cell. Thus, $f$ must be nearly constant inside $\Omega$, and may vanish outside a neighborhood of $\Omega$. From the properties of the Fourier transform, in principle, this implies that $\tilde{f}(\mathbf{k})$ verifies $\tilde{f}(\mathbf{k}) \approx 0$ outside the first Brillouin zone. For example, for the case of simple cubic lattice with lattice constant $a$, the test function may be chosen equal to

$$\begin{aligned} f(\mathbf{r}) &= \left(\pi R^2\right)^{-3/2} e^{-r^2/R^2} \\ \tilde{f}(\mathbf{k}) &= e^{-(kR/2)^2} \end{aligned} \tag{10.14}$$

with $R \approx a$. Such a test function verifies $\tilde{f}(\mathbf{k}) \approx 0$ for points such that $k > \pi/a$.

This discussion shows that it is safe to assume that for $\mathbf{k}$, relatively close to the origin of the Brillouin zone, $\tilde{f}(\mathbf{k}_{\mathbf{J}}) \approx 0$ for $\mathbf{J} \neq 0$ and $\tilde{f}(\mathbf{k}_{\mathbf{J}}) \approx 1$ for $\mathbf{J} = 0$. Thus, by calculating the inverse Fourier transform of Equation 10.13, it follows that

$$\langle\mathbf{E}\rangle \approx \mathbf{E}_{\text{av}} e^{-j\mathbf{k}\cdot\mathbf{r}} \tag{10.15}$$

where $\mathbf{E}_{av}$ is defined as the amplitude of the zero-order Floquet harmonic:

$$\mathbf{E}_{av} = \frac{1}{V_{cell}} \int_{\Omega} \mathbf{E}(\mathbf{r})\, e^{+j\mathbf{k}\cdot\mathbf{r}} d^3\mathbf{r}. \tag{10.16}$$

Proceeding along similar lines and using Equation 10.11, it may be verified that the macroscopic fields, $\langle \mathbf{B} \rangle$ and $\mathbf{D}_g$, verify the formulas*:

$$\langle \mathbf{B} \rangle \approx \mathbf{B}_{av} e^{-j\mathbf{k}\cdot\mathbf{r}}, \quad \mathbf{D}_g \approx \mathbf{D}_{g,av} e^{-j\mathbf{k}\cdot\mathbf{r}} \tag{10.17}$$

where,

$$\mathbf{B}_{av} = \frac{1}{V_{cell}} \int_{\Omega} \mathbf{B}(\mathbf{r})\, e^{+j\mathbf{k}\cdot\mathbf{r}} d^3\mathbf{r} \tag{10.18}$$

$$\mathbf{D}_{g,av} \equiv \varepsilon_0 \mathbf{E}_{av} + \mathbf{P}_{g,av} = \underline{\boldsymbol{\varepsilon}}(\omega, \mathbf{k}) \cdot \mathbf{E}_{av} \tag{10.19}$$

and $\mathbf{P}_{g,av}$ is the generalized polarization vector:

$$\mathbf{P}_{g,av} = \frac{1}{V_{cell} j\omega} \int_{\Omega} \mathbf{J}_d(\mathbf{r})\, e^{+j\mathbf{k}\cdot\mathbf{r}} d^3\mathbf{r} \tag{10.20}$$

As mentioned in Section 10.3.1, $\mathbf{P}_{g,av}$ is closely related to the classic polarization vector. Indeed, if the exponential inside the integral is expanded in powers of the argument, the leading term corresponds exactly to the standard polarization vector (i.e., the average electric dipole moment in a unit cell). The higher-order terms can be related to the magnetization vector and other multipole moments. When the unit cell contains PEC surfaces, the polarization vector may be rewritten as

$$\mathbf{P}_{g,av} = \frac{1}{V_{cell} j\omega} \left( \int_{\partial D} \mathbf{J}_c e^{+j\mathbf{k}\cdot\mathbf{r}} ds + \int_{\Omega - \partial D} \mathbf{J}_d\, e^{+j\mathbf{k}\cdot\mathbf{r}} d^3\mathbf{r} \right) \tag{10.21}$$

where

$\partial D$ is the PEC surface

$\mathbf{J}_c = \hat{\mathbf{v}} \times [\mathbf{B}/\mu_0]$ is the surface current density (see Figure 10.1)

The previous results confirm that provided the test function is properly chosen, the macroscopic fields are completely determined by the amplitudes of the corresponding zero-order Floquet harmonics, as anticipated in the beginning of this section. Moreover, it is proven in Section 10.3.3 that the zero-order harmonics may be used to completely characterize the unknown dielectric function $\underline{\varepsilon}$.

For future reference, it can be verified from the microscopic Maxwell equations (Equation 10.2) that the average fields satisfy exactly the equations:

$$\begin{aligned} -\mathbf{k} \times \mathbf{E}_{av} + \omega \mathbf{B}_{av} &= 0 \\ \omega \left( \varepsilon_0 \mathbf{E}_{av} + \mathbf{P}_{g,av} \right) + \mathbf{k} \times \frac{\mathbf{B}_{av}}{\mu_0} &= -\omega \mathbf{P}_{e,av} \end{aligned} \tag{10.22}$$

where $\mathbf{P}_{e,av} = \frac{1}{V_{cell} j\omega} \int_{\Omega} \mathbf{J}_e e^{+j\mathbf{k}\cdot\mathbf{r}} d^3\mathbf{r}$ is the applied polarization vector.

*Equations 10.15 and 10.17 become exact for $\mathbf{k}$ in the Brillouin zone if one chooses the test function such that $\tilde{f}(\mathbf{k}) = 1$ inside the Brillouin zone and $\tilde{f}(\mathbf{k}) = 0$ outside the Brillouin zone. In such conditions the averaging operator is equivalent to a low pass spatial filter, which retains uniquely the fundamental zero-order Floquet harmonic.

### 10.3.3 Microscopic Theory

We now introduce a microscopic theory based on the constitutive relation (Equation 10.9) that enables the homogenization of arbitrary periodic nonmagnetic materials.

The key idea to retrieve the effective parameters of the periodic medium for fixed $(\omega, \mathbf{k})$ is to excite the structure with a periodic source $\mathbf{J}_e$ that enforces a desired phase modulation in the unit cell, so that the solution $(\mathbf{E}, \mathbf{B})$ of Maxwell equations (Equation 10.2) has the Floquet property. Thus, it is imposed that the applied $\mathbf{J}_e$ has the Floquet property, i.e., $\mathbf{J}_e e^{j\mathbf{k}\cdot\mathbf{r}}$ is periodic in the crystal, where $\mathbf{k}$ is the wave vector associated with the excitation.

From the results of Section 10.3.2 and Equation 10.19, it is known that the dielectric function must verify $\underline{\varepsilon}(\omega, \mathbf{k}) \cdot \mathbf{E}_{av} = \varepsilon_0 \mathbf{E}_{av} + \mathbf{P}_{g,av}$. Hence, for fixed $(\omega, \mathbf{k})$ the dielectric function $\underline{\varepsilon}$ can be completely determined from the previous formula, provided $\mathbf{P}_{g,av}$ is known for three independent vectors $\mathbf{E}_{av}$, e.g., for $\mathbf{E}_{av} \sim \hat{\mathbf{u}}_i$, where $\hat{\mathbf{u}}_i$ is directed along the coordinate axes. Remember that the generalized polarization vector, $\mathbf{P}_{g,av}$, can be computed from the induced microscopic currents.

The specific spatial variation of the chosen applied current $\mathbf{J}_e$, in principle, does not influence significantly the extracted effective parameters, at least if the dimensions of the unit cell are much smaller than the wavelength. However, in view of the hypotheses used in Section 10.3.2 to obtain Equations 10.15 and 10.17, it is desirable that the applied current excites mainly the zero-order Floquet harmonics, and excites as weakly as possible the remaining harmonics. Hence, it is convenient to assume that the applied density of current $\mathbf{J}_e$ is uniform, with $\mathbf{J}_e = \mathbf{J}_{e,av} e^{-j\mathbf{k}\cdot\mathbf{r}}$, where $\mathbf{J}_{e,av}$ is a constant vector independent of $\mathbf{r}$. Using the definition of $\mathbf{P}_{e,av}$, it is seen that the applied current can be written in terms of the applied polarization vector:

$$\mathbf{J}_e = j\omega \mathbf{P}_{e,av} e^{-j\mathbf{k}\cdot\mathbf{r}} \tag{10.23}$$

Thus, the recipe proposed here to calculate the dielectric function can be summarized as follows:

- For fixed $(\omega, \mathbf{k})$, solve the source-driven Maxwell equations (Equation 10.2) for an applied current, as in Equation 10.23, with $\mathbf{P}_{e,av} \sim \hat{\mathbf{u}}_i$, $i = 1, 2, 3$ (or for another equivalent independent set with a dimension three). This involves solving three different source-driven problems.
- From the computed microscopic fields calculate the corresponding macroscopic electric field, $\mathbf{E}_{av}$, and the generalized polarization vector, $\mathbf{P}_{g,av}$.
- Finally, using Equation 10.19, obtain the desired dielectric function $\underline{\varepsilon}$.

It is important to underline that the described method is not based on the solution of an eigenvalue problem, but instead only requires solving Maxwell's equations under a periodic excitation. In particular, the described homogenization procedure can be used to obtain the effective parameters even in frequency band gaps or in case of lossy materials. It should also be clear that the extracted dielectric function is completely independent of the specific test function used to define the macroscopic fields.

In the following sections, it will be illustrated how the outlined method can be applied in practice, and how it can be numerically implemented to homogenize a completely arbitrary microstructured material.

### 10.3.4 Plane Wave Solutions

The dielectric function $\underline{\varepsilon}$ can be used to characterize the Floquet eigenmodes supported by the structured material. In fact, the pair $(\omega, \mathbf{k})$ is associated with an electromagnetic mode of the crystal, if and only if, the Maxwell equations (Equation 10.2) support a $\mathbf{k}$-periodic solution in the absence of an external source, i.e., with $\mathbf{J}_e = 0$. In such a case, the system (Equation 10.22) has a nontrivial solution for $(\mathbf{E}_{av}, \mathbf{B}_{av})$ with an applied polarization vector such that $\mathbf{P}_e = 0$ [30]. Hence, substituting Equation 10.19 into Equation 10.22, it follows that the homogeneous system

$$-\mathbf{k}\times\mathbf{E}_{av}+\omega\mathbf{B}_{av}=0$$
$$\omega\underline{\varepsilon}\cdot\mathbf{E}_{av}+\mathbf{k}\times\frac{\mathbf{B}_{av}}{\mu_0}=0 \tag{10.24}$$

has a nontrivial solution, if and only if $(\omega,\mathbf{k})$ is associated with an electromagnetic mode of the material. This result is exact and valid for arbitrary $(\omega,\mathbf{k})$, not necessarily in the long wavelength limit. In particular, this remarkable property implies that the band structure information of an arbitrary periodic material is completely specified by its dielectric function. Hence, the dielectric function defined, as in Section 10.3.3, can be used to obtain the dispersion diagram and average fields of an arbitrary electromagnetic mode.

The nontrivial solutions of Equation 10.24 determine the plane wave normal modes supported by the homogenized medium. From the previous paragraph, it is evident that there is a one-to-one relation between the Floquet eigenmodes of a structured material and the plane wave normal modes of the corresponding homogenized medium.

From Equation 10.24, it can be proven that the average electric field verifies the characteristic system [4]:

$$\left(\left(\frac{\omega}{c}\right)^2\frac{\underline{\boldsymbol{\varepsilon}}}{\varepsilon_0}+\mathbf{k}\mathbf{k}-k^2\underline{\mathbf{I}}\right)\cdot\mathbf{E}_{av}=\mathbf{0} \tag{10.25}$$

where

$c=1/\sqrt{\varepsilon_0\mu_0}$ is the speed of light in vacuum
$k^2=\mathbf{k}\cdot\mathbf{k}$

After simple manipulations [30], it can be verified that, provided the average field is not transverse, i.e., provided $\mathbf{k}\cdot\mathbf{E}_{av}\neq 0$, the associated wave vector satisfies the characteristic equation:

$$-1=\mathbf{k}\cdot\left(\left(\frac{\omega}{c}\right)^2\frac{\underline{\boldsymbol{\varepsilon}}}{\varepsilon_0}-k^2\underline{\mathbf{I}}\right)^{-1}\cdot\mathbf{k}\quad\text{if}\quad\mathbf{k}\cdot\mathbf{E}_{av}\neq 0 \tag{10.26}$$

The solutions, $\omega=\omega(\mathbf{k})$, of Equation 10.26 yield the dispersion of the plane wave normal modes. The macroscopic average field is given by

$$\mathbf{E}_{av}\propto\left(\frac{\underline{\boldsymbol{\varepsilon}}}{\varepsilon_0}-\frac{c^2k^2}{\omega^2}\underline{\mathbf{I}}\right)^{-1}\cdot\frac{c\mathbf{k}}{\omega}\quad\text{if}\quad\mathbf{k}\cdot\mathbf{E}_{av}\neq 0 \tag{10.27}$$

### 10.3.5 Symmetries of the Dielectric Function

Some relevant properties of the dielectric function are enunciated next [4,30]. Below, the superscript "t" represents the transpose dyadic and the superscript "*" represents complex conjugation.

- $\underline{\varepsilon}(\omega,\mathbf{k})=\underline{\varepsilon}^*(-\omega^*,-\mathbf{k}^*)$.
- $\underline{\varepsilon}(\omega,\mathbf{k})=\underline{\varepsilon}^{\mathrm{t}}(\omega,-\mathbf{k})$.
- Let $\mathbf{T}$ represent a translation. Suppose that a given material is characterized by the dielectric function $\underline{\varepsilon}$, and that the metamaterial resulting from the application of $\mathbf{T}$ to the original structure is characterized by the dielectric function $\underline{\varepsilon}'$. Then, $\underline{\varepsilon}'(\boldsymbol{\omega},\mathbf{k})=\underline{\varepsilon}(\boldsymbol{\omega},\mathbf{k})$. In particular, the definition of the dielectric function is independent of the origin of the coordinate system.
- Let $\mathbf{S}$ be an isometry (a rotation or a reflection): $\mathbf{S}\cdot\mathbf{S}^{\mathrm{t}}=\underline{\mathbf{I}}$. Suppose that a given material is characterized by the dielectric function $\underline{\varepsilon}$, and that the material resulting from the

application of $\mathbf{S}$ to the original structure is characterized by the dielectric function $\underline{\varepsilon}'$. Then, $\underline{\varepsilon}'(\omega, \mathbf{S}\cdot\mathbf{k}) = \mathbf{S}\cdot\underline{\varepsilon}(\omega,\mathbf{k})\cdot\mathbf{S}^{t}$.

- If a material is invariant to the application of an isometry followed by a translation $\mathbf{T}\circ\mathbf{S}$, then its dielectric function satisfies $\underline{\varepsilon}(\omega,\mathbf{S}\cdot\mathbf{k}) = \mathbf{S}\cdot\underline{\varepsilon}(\omega,\mathbf{k})\cdot\mathbf{S}^{t}$. In particular, if the material has a center of inversion symmetry, i.e., the origin can be chosen such that the material is invariant to the inversion $\mathbf{S}:\mathbf{r}\to-\mathbf{r}$, then $\underline{\varepsilon}(\omega,\mathbf{k}) = \underline{\varepsilon}(\omega,-\mathbf{k})$.

## 10.4 Dielectric Function of a Lattice of Electric Dipoles

In order to illustrate the application of the homogenization method introduced in Section 10.3, the dielectric function of a periodic lattice of electric dipoles is characterized next. Besides being of obvious theoretical interest, this canonical problem can be solved in closed analytical form [34], and thus the study of this electromagnetic crystal gives important insights into the homogenization approach. The analysis also yields the generalized Lorentz–Lorenz and Clausius–Mossotti formulas for spatially dispersive media.

It is assumed that the medium consists of a three-dimensional periodic array of identical electric dipoles characterized by the electric polarizability $\underline{\boldsymbol{\alpha}}_{e}$. The dipoles are positioned at the lattice points, $\mathbf{r}_{\mathbf{I}} = i_1\mathbf{a}_1 + i_2\mathbf{a}_2 + i_3\mathbf{a}_3$, where $\mathbf{a}_1$, $\mathbf{a}_2$, and $\mathbf{a}_3$ are the primitive vectors of the crystal, and $\mathbf{I} = (i_1, i_2, i_3)$ is a multi-index of integers.

The microscopic electromagnetic fields induce an electric dipole moment in each particle. The dipole moment $\mathbf{p}_e$ of the particle at the origin is given by

$$\frac{\mathbf{p}_e}{\varepsilon_0} = \underline{\boldsymbol{\alpha}}_e(\omega)\cdot\mathbf{E}_{loc} \tag{10.28}$$

where $\mathbf{E}_{loc}$ is the local electric field that polarizes the inclusion, which is given by the superimposition of the fields radiated by the other particles and the external field.

To calculate the dielectric function of the periodic crystal, we need to solve the Maxwell equations (Equation 10.2) for an applied current of the form given in Equation 10.23. For a lattice of electric dipoles, Equation 10.2 may be rewritten as

$$\begin{aligned}\nabla\times\mathbf{E} &= -j\omega\mathbf{B}\\ \nabla\times\frac{\mathbf{B}}{\mu_0} &= j\omega\mathbf{P}_{e,av}e^{-j\mathbf{k}\cdot\mathbf{r}} + \mathbf{J}_{dip} + j\omega\varepsilon_0\mathbf{E}\end{aligned} \tag{10.29}$$

where $\mathbf{J}_{dip}$ represents the electric microscopic currents induced in the dipoles. Since the applied source has the Floquet property, it is clear that the induced current is such that

$$\mathbf{J}_{dip} = \sum_{\mathbf{I}}\delta(\mathbf{r}-\mathbf{r}_{\mathbf{I}})\,e^{-j\mathbf{k}\cdot\mathbf{r}_{\mathbf{I}}}\,j\omega\mathbf{p}_e \tag{10.30}$$

where

$\mathbf{p}_e$ is the electric dipole moment of the particle at the origin
$\mathbf{r}_{\mathbf{I}}$ represents a generic lattice point
$\delta$ is Dirac's distribution

The solution of Equation 10.29 can be written in a straightforward manner in terms of the lattice Green dyadic, $\underline{\mathbf{G}}_p(\mathbf{r}|\mathbf{r}') = \left(\underline{\mathbf{I}} + \frac{c^2}{\omega^2}\nabla\nabla\right)\Phi_p(\mathbf{r}|\mathbf{r}')$, where $\Phi_p = \Phi_p(\mathbf{r}|\mathbf{r}';\omega,\mathbf{k})$ is the lattice Green function [30,35,36], which verifies

$$\nabla^2\Phi_p + \left(\frac{\omega}{c}\right)^2\Phi_p = -\sum_{\mathbf{I}}\delta(\mathbf{r}-\mathbf{r}'-\mathbf{r}_{\mathbf{I}})e^{-j\mathbf{k}\cdot(\mathbf{r}-\mathbf{r}')} \tag{10.31}$$

In fact, it is simple to confirm that the solution of the problem is

$$\mathbf{E} = (-j\omega\mu_0)\,\underline{\mathbf{G}}_p(\mathbf{r}|\mathbf{0}) \cdot j\omega\mathbf{p}_e + (-j\omega\mu_0)\,V_{\text{cell}}\underline{\mathbf{G}}_{\text{av}} \cdot j\omega\mathbf{P}_{e,\text{av}}e^{-j\mathbf{k}\cdot\mathbf{r}} \tag{10.32}$$

where, by definition,

$$\underline{\mathbf{G}}_{\text{av}} = \frac{1}{V_{\text{cell}}}\int_{\Omega}\underline{\mathbf{G}}_p(\mathbf{r}|\mathbf{r}')\,e^{+j\mathbf{k}\cdot(\mathbf{r}-\mathbf{r}')}\mathrm{d}^3\mathbf{r}' \tag{10.33}$$

From [30], the dyadic $\underline{\mathbf{G}}_{\text{av}}$ and the respective inverse are equal to

$$\begin{aligned}\underline{\mathbf{G}}_{\text{av}} &= \frac{1}{V_{\text{cell}}}\frac{1}{(\omega/c)^2}\frac{(\omega/c)^2\underline{\mathbf{I}} - \mathbf{kk}}{k^2 - (\omega/c)^2}\\ \underline{\mathbf{G}}_{\text{av}}^{-1} &= -V_{\text{cell}}\left[\left((\omega/c)^2 - k^2\right)\underline{\mathbf{I}} + \mathbf{kk}\right]\end{aligned} \tag{10.34}$$

The first term on the right-hand side of Equation 10.32 corresponds to the field created by the induced electric dipoles, and the second term corresponds to the field created by the applied source, $\mathbf{P}_{e,\text{av}}$.

To obtain the full solution of Equation 10.29, it is still necessary to determine the unknown, $\mathbf{p}_e$. From Equation 10.32 it is obvious that the local electric field that polarizes the particle at the origin is

$$\mathbf{E}_{\text{loc}} = \left(\frac{\omega}{c}\right)^2\underline{\mathbf{G}}'_p(\mathbf{0}|\mathbf{0}) \cdot \frac{\mathbf{p}_e}{\varepsilon_0} + \left(\frac{\omega}{c}\right)^2 V_{\text{cell}}\underline{\mathbf{G}}_{\text{av}} \cdot \frac{\mathbf{P}_{e,\text{av}}}{\varepsilon_0} \tag{10.35}$$

where, by definition,

$$\underline{\mathbf{G}}'_p(\mathbf{r}|\mathbf{r}') = \underline{\mathbf{G}}_p(\mathbf{r}|\mathbf{r}') - \underline{\mathbf{G}}_f(\mathbf{r}|\mathbf{r}') \tag{10.36}$$

and $\underline{\mathbf{G}}_f(\mathbf{r}|\mathbf{r}')$ is the free-space Green-dyadic for a single electric dipole with the Sommerfeld radiation conditions. The electric dipole moment $\mathbf{p}_e$ can now be obtained as a function of the excitation by substituting Equation 10.28 into Equation 10.35, and solving the resulting equation for $\mathbf{p}_e$. This gives the formal solution of the microscopic equations (Equation 10.29).

To obtain the dielectric function of the crystal, it is necessary to link the polarization vector, $\mathbf{P}_{g,\text{av}}$, with the macroscopic field, $\mathbf{E}_{\text{av}}$. The vector $\mathbf{P}_{g,\text{av}}$ can be obtained by substituting Equation 10.30 into Equation 10.20. As could be expected, the following relation holds:

$$\mathbf{P}_{g,\text{av}} = \frac{\mathbf{p}_e}{V_{\text{cell}}} \tag{10.37}$$

On the other hand, the induced average electric field can be related to the applied polarization vector using the relations given in Equation 10.22. Straightforward calculations demonstrate that

$$\frac{\mathbf{P}_{e,\text{av}}}{\varepsilon_0} + \frac{\mathbf{P}_{g,\text{av}}}{\varepsilon_0} = \frac{c^2}{\omega^2}\frac{1}{V_{\text{cell}}}\underline{\mathbf{G}}_{\text{av}}^{-1} \cdot \mathbf{E}_{\text{av}} \tag{10.38}$$

Using the previous relations in Equation 10.35, it is found that the local field can be rewritten as

$$\mathbf{E}_{\text{loc}} = \mathbf{E}_{\text{av}} + \underline{\mathbf{C}}_i(\omega,\mathbf{k}) \cdot \frac{\mathbf{p}_e}{\varepsilon_0} \tag{10.39}$$

where the interaction dyadic $\underline{\mathbf{C}}_i$ is, by definition,

$$\underline{\mathbf{C}}_i(\omega,\mathbf{k}) = \left(\frac{\omega}{c}\right)^2\left(\underline{\mathbf{G}}'_p(\mathbf{0}|\mathbf{0};\omega,\mathbf{k}) - \underline{\mathbf{G}}_{\text{av}}(\omega,\mathbf{k})\right) \tag{10.40}$$

Equation 10.39 relates the local field with the macroscopic field and the induced dipole moment. This important relation is a generalization of the classical Lorentz–Lorenz formula [12]. It describes the effect of frequency dispersion, as well as of spatial dispersion, which may emerge due to the noncontinuous (discrete) nature of the material.

Using the generalized Lorentz–Lorenz formula, it is simple to obtain the dielectric function of the composite material. Substituting Equations 10.28 and 10.37 into Equation 10.39, it is found that

$$(\underline{\mathbf{I}} - \underline{\boldsymbol{\alpha}}_e \cdot \underline{\mathbf{C}}_{\mathrm{i}}) \cdot \frac{\mathbf{P}_{\mathrm{g,av}}}{\varepsilon_0} = \frac{1}{V_{\mathrm{cell}}} \underline{\boldsymbol{\alpha}}_e \cdot \mathbf{E}_{\mathrm{av}} \tag{10.41}$$

Solving the above equation for $\mathbf{P}_{\mathrm{g,av}}$ and using Equation 10.19, it clear that the dielectric function of the lattice of dipoles is given by

$$\underline{\boldsymbol{\varepsilon}}(\omega, \mathbf{k}) = \underline{\mathbf{I}} + \frac{1}{V_{\mathrm{cell}}} \left(\underline{\mathbf{I}} - \underline{\boldsymbol{\alpha}}_e \cdot \underline{\mathbf{C}}_{\mathrm{i}}(\omega, \mathbf{k})\right)^{-1} \cdot \underline{\boldsymbol{\alpha}}_e \tag{10.42}$$

This is an important result and also generalization of the classical Clausius–Mossotti formula [12]. It establishes that the dielectric function can be written in terms of the electric polarizability of the particles and of the interaction dyadic $\underline{\mathbf{C}}_{\mathrm{i}}$. It is stressed that the above result is exact within the theory described in Section 10.3. In particular, the dispersion characteristic of the electromagnetic modes may be obtained by substituting the dielectric function into Equation 10.24, and by calculating the values of $(\omega, \mathbf{k})$ for which the homogeneous system has nontrivial solutions.

It can be proven that in the quasistatic limit, the interaction dyadic of a simple cubic lattice is given by [34]

$$\underline{\mathbf{C}}_{\mathrm{i}}(\omega = 0, \mathbf{k} = \mathbf{0}) = \frac{1}{3V_{\mathrm{cell}}} \underline{\mathbf{I}} \qquad \text{(s.c. lattice)} \tag{10.43}$$

In the general dynamical case, $\underline{\mathbf{C}}_{\mathrm{i}}$ has to be evaluated numerically. For more details the reader is referred to [34]. The imaginary part of the interaction dyadic can always be evaluated in closed analytical form. Detailed calculations show that [34]

$$\mathrm{Im}\left\{\underline{\mathbf{C}}_{\mathrm{i}}(\omega, \mathbf{k})\right\} = \frac{1}{6\pi} \left(\frac{\omega}{c}\right)^3 \underline{\mathbf{I}} \tag{10.44}$$

This property implies that if the particles are lossless, the dielectric function is real-valued. In fact, it is known that in order that the balance between the power radiated by the electric dipole and the power absorbed from the local field be zero, it is necessary that the electric polarizability verifies $\mathrm{Im}\left\{\underline{\boldsymbol{\alpha}}_{\mathrm{e}}^{-1}\right\} = \frac{1}{6\pi}\left(\frac{\omega}{c}\right)^3 \underline{\mathbf{I}}$ (it is assumed without loss of generality that $\underline{\boldsymbol{\alpha}}_{\mathrm{e}}$ has an inverse). This property is sometimes reffered to as the Sipe–Kranendonk condition [3]. Using this power balance consistency condition and Equation 10.44, it follows that in the lossless care the dielectric function may be rewritten as

$$\underline{\boldsymbol{\varepsilon}}(\omega, \mathbf{k}) = \underline{\mathbf{I}} + \frac{1}{V_{\mathrm{cell}}} \left(\mathrm{Re}\left\{\underline{\boldsymbol{\alpha}}_e^{-1} - \underline{\mathbf{C}}_{\mathrm{i}}(\omega, \mathbf{k})\right\}\right)^{-1} \tag{10.45}$$

Thus, the dielectric function is real-valued, consistently with what could be expected for a lossless medium with a center of inversion symmetry, and that supports electromagnetic modes that propagate coherently with no radiation loss. An alternative proof of these properties is presented in [24]. The application of the theory to a lattice of split-ring resonators is described in [25].

## 10.5 Numerical Calculation of the Dielectric Function of a Structured Material

Here, it is explained how the homogenization approach introduced in Section 10.3 can be numerically implemented to characterize arbitrary microstructured materials using computational methods. To this end, we will derive an equivalent regularized formulation of the homogenization problem that is suitable for the numerical implementation of the method using MoM.

### 10.5.1 Regularized Formulation

The direct homogenization approach described in Section 10.3.3 may not be adequate for the numerical extraction of the dielectric function. The problem is that when $(\omega, \mathbf{k})$ is associated with an electromagnetic mode of the periodic medium, in general, the source-driven problem (Equation 10.2) cannot be solved because the corresponding homogeneous system (with $\mathbf{J}_e = 0$) has a nontrivial solution. The physical reason for the lack of solution is that when the medium is excited with a source associated with the same $(\omega, \mathbf{k})$ as an eigenmode, the amplitude of the induced fields may grow without limit due to resonant effects. Thus, the direct approach of Section 10.3.3 cannot be applied to calculate the dielectric function when $(\omega, \mathbf{k})$ belongs to the band structure of the material. This is an undesired property because the effective parameters of a composite medium are intrinsically related to the electromagnetic modes.

Since $\underline{\varepsilon}(\omega, \mathbf{k})$ is, in principle, an analytic function of its arguments, this problem could be solved by calculating the dielectric function using a limit procedure. However, in general, the band structure of the composite material is not known a priori, and even if it were known the calculation of the dielectric function at points very close to the band diagram may be numerically unstable.

To circumvent this drawback, a regularized formulation of the homogenization problem is presented next. The basic idea is to tune the applied current $\mathbf{J}_e$ in such a way that the microscopic electric field has a given desired average value $\mathbf{E}_{av}$, preventing in this way the excitation of a resonance when $(\omega, \mathbf{k})$ is associated with an eigenmode. This is possible because the amplitude of $\mathbf{J}_e$ becomes interrelated with the induced microscopic currents in the periodic medium, in such a way that depolarization effects prevent the fields in the medium to grow without limit when a resonance is approached.

To put these ideas into a firm mathematical basis, we will first relate the amplitude of $\mathbf{J}_e$ with the macroscopic field $\mathbf{E}_{av}$. To this end, we use Equation 10.22 to find that the applied polarization vector may be written in terms of the macroscopic electric field and of the polarization vector as

$$\frac{\mathbf{P}_{e,av}}{\varepsilon_0} = \frac{c^2}{\omega^2}\frac{1}{V_{cell}}\underline{\mathbf{G}}^{-1}_{av}\cdot\mathbf{E}_{av} - \frac{\mathbf{P}_{g,av}}{\varepsilon_0} \tag{10.46}$$

where $\underline{\mathbf{G}}^{-1}_{av}$ is defined as in Equation 10.34. It is convenient to rewrite the above equation in terms of two auxiliary operators $\hat{\mathbf{P}}$ and $\hat{\mathbf{P}}_{av}$. The polarization operator, $\hat{\mathbf{P}}$, transforms the electric field into the corresponding (generalized) polarization vector, $\hat{\mathbf{P}} : \mathbf{E} \to \mathbf{P}_{g,av} = \hat{\mathbf{P}}(\mathbf{E})$, where

$$\frac{\hat{\mathbf{P}}(\mathbf{E})}{\varepsilon_0} = \frac{1}{V_{cell}}\left(\frac{c^2}{\omega^2}\int_{\partial D}\hat{\mathbf{v}}\times\left[\nabla\times\mathbf{E}\right]e^{+j\mathbf{k}\cdot\mathbf{r}}ds + \int_{\Omega-\partial D}(\varepsilon_r - 1)\ \mathbf{E}\ e^{+j\mathbf{k}\cdot\mathbf{r}}d^3\mathbf{r}\right) \tag{10.47}$$

In the above, $\left[\nabla\times\mathbf{E}\right] = \nabla\times\mathbf{E}^+ - \nabla\times\mathbf{E}^-$ stands for the discontinuity of the curl of $\mathbf{E}$ at the metallic surfaces, and $\nabla\times\mathbf{E}^+$ is evaluated at the outer side of $\partial D$ (Figure 10.1). It can be easily verified that the above definition is consistent with Equation 10.21. The second operator, $\hat{\mathbf{P}}_{av}$, acts on constant vectors (not on vector fields), $\hat{\mathbf{P}}_{av} : \mathbf{E}_{av} \to \hat{\mathbf{P}}_{av}(\mathbf{E}_{av})$, and is given by

$$\frac{\hat{\mathbf{P}}_{\text{av}}(\mathbf{E}_{\text{av}})}{\varepsilon_0} = \frac{c^2}{\omega^2}\frac{1}{V_{\text{cell}}}\underline{\mathbf{G}}_{\text{av}}^{-1}\cdot\mathbf{E}_{\text{av}} \tag{10.48}$$

Equation 10.46 is thus equivalent to

$$\mathbf{P}_{\text{e,av}} = \hat{\mathbf{P}}_{\text{av}}(\mathbf{E}_{\text{av}}) - \hat{\mathbf{P}}(\mathbf{E}) \tag{10.49}$$

Using the definition of $\mathbf{P}_{\text{e,av}}$ and Equation 10.23, it is found that applied density of current is such that

$$\mathbf{J}_{\text{e}} = j\omega\left(\hat{\mathbf{P}}_{\text{av}}(\mathbf{E}_{\text{av}}) - \hat{\mathbf{P}}(\mathbf{E})\right)e^{-j\mathbf{k}\cdot\mathbf{r}} \tag{10.50}$$

In particular, this formula shows that the applied current density can be regarded as a function of the induced macroscopic field $\mathbf{E}_{\text{av}}$. Thus, to impose the desired macroscopic field $\mathbf{E}_{\text{av}}$, we can excite the material with an applied current of the form given in Equation 10.50. Notice that in such a case $\mathbf{J}_{\text{e}}$ is also a function of the unknown microscopic field $\mathbf{E}$. Such a feedback mechanism prevents a resonance from being excited when $(\omega, \mathbf{k})$ is associated with an electromagnetic mode.

To clarify the discussion, we substitute Equation 10.50 into Maxwell's equations (Equation 10.2) to obtain

$$\begin{aligned}\nabla\times\mathbf{E} &= -j\omega\mathbf{B}\\ \nabla\times\frac{\mathbf{B}}{\mu_0} &= j\omega\left(\hat{\mathbf{P}}_{\text{av}}(\mathbf{E}_{\text{av}}) - \hat{\mathbf{P}}(\mathbf{E})\right)e^{-j\mathbf{k}\cdot\mathbf{r}} + \varepsilon_0\varepsilon_{\text{r}}j\omega\,\mathbf{E}\end{aligned} \tag{10.51}$$

The above system is, by definition, the regularized formulation of the homogenization problem. Even though it is closely related with the original set of equations (Equation 10.2), there are some important differences. First of all, unlike the direct approach (Equation 10.2), Equation 10.51 is an integral–differential system, i.e., both differential operators $(\nabla\times)$ and integral operators $(\hat{\mathbf{P}}(.))$ act on the electromagnetic fields. Note that $\hat{\mathbf{P}}(.)$ yields the generalized polarization of the unknown field $\mathbf{E}$, which involves the integration of the electric field over the unit cell.

A fundamental difference between the direct and regularized formulations is that while in the direct approach the source of fields is $\mathbf{J}_{\text{e}}$, in regularized formulation the source of fields is (from a mathematical point of view) the constant vector $\mathbf{E}_{\text{av}}$. Thus, the solutions of the homogeneous problem $(\mathbf{J}_{\text{e}} = 0)$ associated with the direct problem (Equation 10.2) are different from the solutions of the homogeneous system $(\mathbf{E}_{\text{av}} = 0)$ associated with the regularized system (Equation 10.51), i.e., the two systems have different null spaces. In particular, the electromagnetic modes of the periodic medium are, in general, associated with a nontrivial $\mathbf{E}_{\text{av}}$ and so, do not belong to the null space of the regularized problem. Thus, the regularized formulation can be used to compute the effective parameters of the composite medium even if $(\omega, \mathbf{k})$ is associated with an electromagnetic mode. In fact, when $(\omega, \mathbf{k})$ is associated with a modal solution, we have, $\hat{\mathbf{P}}_{\text{av}}(\mathbf{E}_{\text{av}}) = \hat{\mathbf{P}}(\mathbf{E})$, and thus, the amplitude of the imposed current in Equation 10.51 vanishes, avoiding the excitation of the resonance. However, since $\mathbf{E}_{\text{av}}$ is different from zero, Equation 10.51 still represents a well-formulated source-driven problem.

It is stressed that the effective parameters retrieved by solving the direct problem (Equation 10.2) are exactly the same as those obtained by solving Equation 10.51. The only difference between the two formulations is that the regularized formulation can be applied even when $(\omega, \mathbf{k})$ is associated with an electromagnetic mode. The price that we have to pay for this property is the increased complexity of integral–differential system (Equation 10.51) as compared to the simpler differential system (Equation 10.2). However, as described in Section 10.5.2, the regularized problem can be solved very efficiently using integral equation methods.

### 10.5.2 Integral Equation Solution

It can be verified that for given $(\mathbf{E}_{\text{av}}, \omega, \mathbf{k})$ the solution of the regularized homogenization problem (Equation 10.51) has the integral representation [30]:

$$\mathbf{E}(\mathbf{r}) = \mathbf{E}_{\text{av}} e^{-j\mathbf{k}\cdot\mathbf{r}} + \int_{\partial D} \underline{\mathbf{G}}_{p0}(\mathbf{r}|\mathbf{r}') \cdot (\hat{\mathbf{v}}' \times [\nabla' \times \mathbf{E}])\, \mathrm{d}s'$$
$$+ \int_{\Omega - \partial D} \underline{\mathbf{G}}_{p0}(\mathbf{r}|\mathbf{r}') \cdot \left(\frac{\omega}{c}\right)^2 (\varepsilon_r(\mathbf{r}') - 1)\, \mathbf{E}(\mathbf{r}')\, \mathrm{d}^3\mathbf{r}' \tag{10.52}$$

where $\underline{\mathbf{G}}_{p0}$ is the Green function dyadic defined by

$$\underline{\mathbf{G}}_{p0} = \left(\underline{\mathbf{I}} + \frac{c^2}{\omega^2}\nabla\nabla\right) \Phi_{p0}$$
$$\Phi_{p0}(\mathbf{r}|\mathbf{r}') = \Phi_p(\mathbf{r}|\mathbf{r}') - \frac{1}{V_{\text{cell}}} \frac{e^{-j\mathbf{k}\cdot(\mathbf{r}-\mathbf{r}')}}{k^2 - \omega^2/c^2} \tag{10.53}$$

and $\mathbf{\Phi}_p$ is the lattice Green function that verifies Equation 10.31. The integral representation (Equation 10.52) establishes that the microscopic field **E** can be written in terms of the induced microscopic currents and of the macroscopic electric field.

This is an important result and can be used to reduce the homogenization problem to a standard integral equation with unknowns given by the microscopic currents, $\mathbf{J}_{\text{d}} = \varepsilon_0(\varepsilon_{\text{r}} - 1)\, j\omega\mathbf{E}$, at the dielectric inclusions, $\mathbf{J}_{\text{c}} = \hat{\mathbf{v}} \times [\mathbf{B}]/\mu_0$, at the PEC surfaces. To illustrate this fact, it is considered next that the periodic medium is purely dielectric. In that case, the unknown of the integral equation may be taken equal to the vector field, $\mathbf{f} = (\varepsilon_{\text{r}} - 1)\mathbf{E}$. Notice that the vector density **f** vanishes in the host medium and is proportional to the microscopic current $\mathbf{J}_{\text{d}}$. The integral equation is obtained by imposing that Equation 10.52 is verified at the dielectric inclusions:

$$\frac{\mathbf{f}(\mathbf{r})}{\varepsilon_{\text{r}}(\mathbf{r}) - 1} = \mathbf{E}_{\text{av}} e^{-j\mathbf{k}\cdot\mathbf{r}} + \left(\frac{\omega}{c}\right)^2 \int_{\Omega} \underline{\mathbf{G}}_{p0}(\mathbf{r}|\mathbf{r}') \cdot \mathbf{f}(\mathbf{r}')\, \mathrm{d}^3\mathbf{r}' \tag{10.54}$$

The above identity is valid in the dielectric support of the inclusions, $\{\mathbf{r} : \varepsilon_{\text{r}}(\mathbf{r}) - 1 \neq 0\}$. For a given $\mathbf{E}_{\text{av}}$, this integral equation can be discretized and numerically solved with respect to **f** using standard techniques. In what follows, we briefly review the solution of the problem using MoM [37].

To apply the MoM, **f** is expanded in terms of expansion functions $\mathbf{w}_1, \mathbf{w}_2, \ldots, \mathbf{w}_n, \ldots$:

$$\mathbf{f} = \sum_n c_n \mathbf{w}_n \tag{10.55}$$

The set of expansion functions is assumed complete in $\{\mathbf{r} : \varepsilon_{\text{r}}(\mathbf{r}) - 1 \neq 0\}$. From the definition it is obvious that **f** is a Floquet field, i.e., $\mathbf{f}\exp(j\mathbf{k}\cdot\mathbf{r})$ is periodic. Thus, in general, the expansion functions must have the same property and, therefore, must depend explicitly on **k**, i.e., $\mathbf{w}_n = \mathbf{w}_{n,\mathbf{k}}(\mathbf{r})$. The dependence on **k** can be suppressed only if the inclusions are nonconnected [30].

For a given $\mathbf{E}_{\text{av}}$, the unknown coefficients, $c_n$, can be obtained by substituting the expansion Equation 10.55 into the integral equation (Equation 10.54), and by testing the resulting identity with appropriate test functions. Once **f** has been determined, we can compute the generalized polarization vector using Equation 10.20, and the dielectric function using Equation 10.19. The details can be read in [30]. It is found that the dielectric function can be written as

$$\frac{\underline{\boldsymbol{\varepsilon}}}{\varepsilon_0}(\omega, \mathbf{k}) = \underline{\mathbf{I}} + \frac{1}{V_{\text{cell}}} \sum_{m,n} \chi^{m,n} \left(\int_{\Omega} \mathbf{w}_{m,\mathbf{k}}(\mathbf{r})\, e^{+j\mathbf{k}\cdot\mathbf{r}} \mathrm{d}^3\mathbf{r}\right) \otimes \left(\int_{\Omega} \mathbf{w}_{n,-\mathbf{k}}(\mathbf{r})\, e^{-j\mathbf{k}\cdot\mathbf{r}} \mathrm{d}^3\mathbf{r}\right) \tag{10.56}$$

where

⊗ denotes the tensor product of two vectors

$\chi^{m,n}$ is an element of the infinite matrix $[\chi^{m,n}]$, whose inverse $[\chi_{m,n}]$ has a generic element given by

$$\chi_{m,n} = \int_{\Omega} \frac{1}{\varepsilon_r(\mathbf{r}) - 1} \mathbf{w}_{m,-\mathbf{k}}(\mathbf{r}) \cdot \mathbf{w}_{n,\mathbf{k}}(\mathbf{r})\, d^3\mathbf{r} - \left(\frac{\omega}{c}\right)^2 \int_{\Omega}\int_{\Omega} \mathbf{w}_{m,-\mathbf{k}}(\mathbf{r}) \cdot \underline{\mathbf{G}}_{p0}(\mathbf{r}|\mathbf{r}') \cdot \mathbf{w}_{n,\mathbf{k}}(\mathbf{r}')\, d^3\mathbf{r}\, d^3\mathbf{r}' \tag{10.57}$$

Since the expansion functions must vanish outside the dielectric inclusions, the integration domain in the above integrals may be replaced by $\{\mathbf{r} \in \Omega : \varepsilon_r(\mathbf{r}) - 1 \neq 0\}$. The above formulas are valid for dielectric crystals with no PEC surfaces.

Equation 10.56 establishes that the dielectric function of the periodic material can be written exclusively in terms of the expansion functions, $\mathbf{w}_{n,\mathbf{k}}$, and of the Green dyadic, $\underline{\mathbf{G}}_{p0}$. This formula is extremely useful for the numerical evaluation of the effective parameters of composite materials, and its application is illustrated in the following sections.

In case the material contains only PEC surfaces and $\varepsilon_r - 1 = 0$ in the unit cell, the unknown of the integral equation is taken equal to the vector tangential density, $\mathbf{f} = \frac{c^2}{\omega^2}\hat{\mathbf{v}}' \times [\nabla' \times \mathbf{E}]$, defined over the metallic surface $\partial D$. The vector field $\mathbf{f}$ is proportional to the density of current $\mathbf{J}_c$. As in the dielectric case, the unknown is expanded in terms of the complete set of vectors $\mathbf{w}_1$, $\mathbf{w}_2$, ..., except that now the expansion functions form a complete set of tangential vector fields over the metallic surface. A detailed analysis [30] shows that the dielectric function of such a material is given by

$$\frac{\underline{\boldsymbol{\varepsilon}}}{\varepsilon_0}(\omega, \mathbf{k}) = \underline{\mathbf{I}} + \frac{1}{V_{\text{cell}}} \sum_{m,n} \chi^{m,n} \left(\int_{\partial D} \mathbf{w}_{m,\mathbf{k}}(\mathbf{r})\, e^{+j\mathbf{k}\cdot\mathbf{r}} ds\right) \otimes \left(\int_{\partial D} \mathbf{w}_{n,-\mathbf{k}}(\mathbf{r})\, e^{-j\mathbf{k}\cdot\mathbf{r}} ds\right) \tag{10.58}$$

$$\chi_{m,n} = \int_{\partial D}\int_{\partial D} \left(\nabla_s \cdot \mathbf{w}_{m,-\mathbf{k}}(\mathbf{r})\, \nabla'_s \cdot \mathbf{w}_{n,\mathbf{k}}(\mathbf{r}') - \frac{\omega^2}{c^2} \mathbf{w}_{m,-\mathbf{k}}(\mathbf{r}) \cdot \mathbf{w}_{n,\mathbf{k}}(\mathbf{r}')\right) \Phi_{p0}(\mathbf{r}|\mathbf{r}')\, ds\, ds' \tag{10.59}$$

where

$\nabla_s \cdot$ represents the surface divergence of a tangential vector field

the matrix $[\chi^{m,n}]$ is the inverse of $[\chi_{m,n}]$

### 10.5.3 Application to Wire Media

To illustrate the versatility and usefulness of the formalism derived in Section 10.5.2, here we characterize the dielectric function of a square array of metallic rods (wire medium). Such a material is characterized by strong spatial dispersion, even in the long wavelength limit [20]. To give an intuitive physical picture of this phenomenon and understand its origin, consider an arbitrary metallic wire in an electromagnetic crystal. Since the wire is a good conductor, the current that flows along the wire at a given point, depends not only on the microscopic electric field in the immediate vicinity of the considered point, but also on the distribution of the electric field in the neighborhood of the whole wire axis. In fact, since the electric current along the wire must be continuous, it is clear that a localized fluctuation of the electric field may be propagated to a considerable distance from the perturbation point by current carriers. Hence, the radius of action of the microscopic electric field on the current along the wire may be much larger than the lattice constant, which defines the characteristic dimension of the wire medium, and possibly comparable or larger than the wavelength of

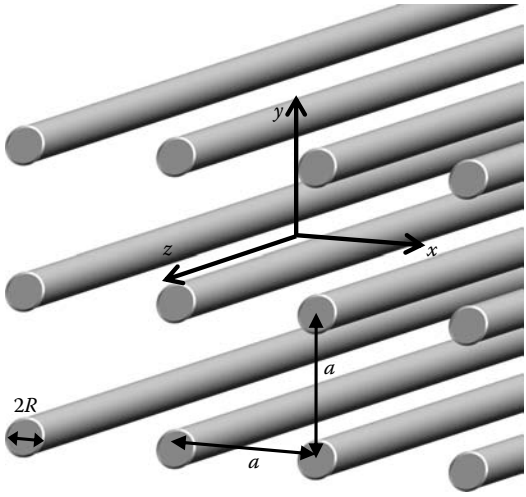


**FIGURE 10.2** The wire medium is formed by a square array of infinitely long metallic rods oriented along the $z$-direction. (Reprinted from Silveirinha, M.G., Belov, P.A., and Simovski, C.R., *Phys. Rev. B*, 75, 035108, 2007. With permission.)

radiation. This phenomenon is, in many ways, analogous to a slow diffusion effect, because the velocity of the current carriers is much slower than the velocity of photons. Since the polarization vector **P** is proportional to the current along the wire, it follows that this long range slow diffusion effect is the origin of the nonlocal properties of the wire medium.

In order to characterize the spatial dispersion effects in wire media, we consider the geometry of Figure 10.2. The lattice constant is $a$ and the radius of the rods is $R$. We suppose that $R/a \ll 1$ so that the thin-wire approximation can be used. Within such approximation, it is legitimate to assume that the surface current is uniform in the cross section of the wires and flows exclusively along the axes of the rods. Thus, since the structure is uniform along the $z$-direction, it follows that one single expansion function is sufficient to describe the behavior of the induced surface current density, $\mathbf{J}_c$, for an excitation with Floquet spatial variation, as in Equation 10.23. The expansion function may be taken equal to

$$\mathbf{w}_{1,\mathbf{k}}(\mathbf{r}) = \frac{e^{-j\mathbf{k}\cdot\mathbf{r}}}{2\pi R}\hat{\mathbf{u}}_z \tag{10.60}$$

Using this expression in Equation 10.58, it is found that the dielectric function of the wire medium is given by

$$\frac{\underline{\boldsymbol{\varepsilon}}}{\varepsilon_0}(\omega,\mathbf{k}) = \underline{\mathbf{I}} + \frac{1}{V_{\text{cell}}}\frac{a^2}{\chi_{11}(\omega,\mathbf{k})}\hat{\mathbf{u}}_z\hat{\mathbf{u}}_z \tag{10.61}$$

where $\chi_{11}$ is calculated using Equation 10.59, and is given by

$$\chi_{11}(\omega,\mathbf{k}) = \left(k_z^2 - \frac{\omega^2}{c^2}\right)\frac{1}{(2\pi R)^2}\int_{\partial D}\int_{\partial D}\Phi_{p0}(\mathbf{r}|\,\mathbf{r}';\omega,\mathbf{k})\,e^{j\mathbf{k}\cdot(\mathbf{r}-\mathbf{r}')}\mathrm{d}s\mathrm{d}s' \tag{10.62}$$

and $\partial D = \left\{(x,y,z) : x^2 + y^2 = R^2, -a/2 < z < a/2\right\}$ represents the surface of the metallic wire in the unit cell. Substituting the above expression into Equation 10.61, the dielectric function can be rewritten as

$$\frac{\underline{\boldsymbol{\varepsilon}}}{\varepsilon_0}(\omega,\mathbf{k}) = \underline{\mathbf{I}} - \frac{\beta_p^2}{\omega^2/c^2 - k_z^2}\hat{\mathbf{u}}_z\hat{\mathbf{u}}_z \tag{10.63}$$

where the plasma wave number $\beta_p$ is such that

$$\frac{1}{\beta_p^2} = \frac{a}{(2\pi R)^2} \int_{\partial D} \int_{\partial D} \Phi_{p0}(\mathbf{r}|\mathbf{r}'; \omega, \mathbf{k})\, e^{j\mathbf{k}\cdot(\mathbf{r}-\mathbf{r}')} ds ds' \tag{10.64}$$

As it is manifest from the above expression, in general, the plasma wave number depends on both ω and **k**, or more specifically, it depends on ω, $k_x$, and $k_y$ (but not on $k_z$). However, in the long wavelength limit, it is an excellent approximation to assume that $\beta_p \approx \beta_p\big|_{\substack{\omega=0 \\ k_x=k_y=0}}$, which may be explicitly evaluated in terms of Bessel functions as in formula (B5) of [23]. Such a formula is equivalent to the result reported in [20]:

$$(\beta_p a)^2 = \frac{2\pi}{\ln\left(\frac{a}{2\pi R}\right) + 0.5275} \tag{10.65}$$

Equations 10.63 and 10.65 determine the dielectric function of the wire medium in the long wavelength limit. For more details about the electrodynamics of wire media and the effect of strong spatial dispersion the reader is referred to [20].

The previous analysis shows that the theory described in Section 10.5.2 can be used to obtain in a very straightforward manner the homogenization model originally derived in [20] using a less direct approach. This demonstrates that the formalism of Section 10.5.2 can be applied not only to calculate the dielectric function using numerical methods, but also to derive approximate analytical models. Such a potential is further demonstrated in [38], where the dielectric function of a square array of helical wires is calculated using similar analytical methods.

## 10.6 Extraction of the Local Parameters from the Nonlocal Dielectric Function

Even though the formalism described in Section 10.3 deals with the characterization of spatially dispersive materials, it is possible to extract the local effective parameters associated with the model (Equation 10.6) (if meaningful) from the nonlocal dielectric function. Such ideas are developed in this section.

### 10.6.1 Relation between the Local and Nonlocal Effective Parameters

In most of the works on metamaterials, the composite structures are characterized using an effective permittivity and an effective permeability. It is, thus, relevant to study the relation between the nonlocal dielectric function and the local parameters. To derive such a relation, we remember that the generalized polarization vector $\mathbf{P}_g$ can be expanded as in Equation 10.8. Calculating the spatial Fourier transform of that formula and using the nonlocal constitutive relations (Equation 10.11), it is found that

$$\tilde{\mathbf{P}}_g = (\underline{\boldsymbol{\varepsilon}}(\omega, \mathbf{k}) - \varepsilon_0 \underline{\mathbf{I}}) \cdot \langle \tilde{\mathbf{E}} \rangle = \tilde{\mathbf{P}} - \frac{\mathbf{k}}{\omega} \times \tilde{\mathbf{M}} + \cdots \tag{10.66}$$

where the symbol "~" represents the Fourier transformation. The terms omitted on the right-hand side of the second identity are related to the quadrupole moment and other higher-order multipoles, and thus, are in general negligible. In a local material the polarization and magnetization vectors, **P** and **M**, can be easily related to the local effective parameters and macroscopic fields using Equations 10.5 and 10.6:

$$\mathbf{P} = \varepsilon_0 \left(\underline{\varepsilon}_r - \underline{\mathbf{I}}\right) \cdot \langle \mathbf{E} \rangle + \frac{1}{\mu_0 c}\, \underline{\boldsymbol{\xi}} \cdot \underline{\boldsymbol{\mu}}_r^{-1} \cdot \left( \langle \mathbf{B} \rangle - \frac{1}{c} \underline{\boldsymbol{\zeta}} \cdot \langle \mathbf{E} \rangle \right)$$

$$\mathbf{M} = \frac{1}{\mu_0 c}\, \underline{\boldsymbol{\mu}}_r^{-1} \cdot \underline{\boldsymbol{\zeta}} \cdot \langle \mathbf{E} \rangle + \frac{1}{\mu_0} \left( \underline{\mathbf{I}} - \underline{\boldsymbol{\mu}}_r^{-1} \right) \cdot \langle \mathbf{B} \rangle \tag{10.67}$$

Calculating the Fourier transform of the above expressions, using the relation $\langle \tilde{\mathbf{B}} \rangle = \frac{\mathbf{k}}{\omega} \times \langle \tilde{\mathbf{E}} \rangle$, substituting the resulting formulas into Equation 10.66, and noting that the obtained equation must hold for arbitrary $\langle \tilde{\mathbf{E}} \rangle$, it is found that

$$\frac{\underline{\boldsymbol{\varepsilon}}}{\varepsilon_0}(\omega, \mathbf{k}) = \left(\underline{\varepsilon}_r - \underline{\boldsymbol{\xi}} \cdot \underline{\boldsymbol{\mu}}_r^{-1} \cdot \underline{\boldsymbol{\zeta}}\right) + \left(\underline{\boldsymbol{\xi}} \cdot \underline{\boldsymbol{\mu}}_r^{-1} \times \frac{c\mathbf{k}}{\omega} - \frac{c\mathbf{k}}{\omega} \times \underline{\boldsymbol{\mu}}_r^{-1} \cdot \underline{\boldsymbol{\zeta}}\right) + \frac{c\mathbf{k}}{\omega} \times \left(\underline{\boldsymbol{\mu}}_r^{-1} - \underline{\mathbf{I}}\right) \times \frac{c\mathbf{k}}{\omega} \tag{10.68}$$

This expression gives the desired relation between the nonlocal dielectric function and the local effective parameters. Thus, a local material can be characterized using the nonlocal constitutive relations (Equation 10.11) as well as using the local constitutive relations (Equation 10.6) being the corresponding effective parameters linked as in Equation 10.68. For local materials, the two phenomenological models are perfectly equivalent: they predict exactly the same dispersion characteristic, $\omega = \omega(\mathbf{k})$, for plane wave modes, and the same macroscopic fields, $\mathbf{E}_{av}$ and $\mathbf{B}_{av}$. In particular, it is clear that the dielectric function, $\underline{\varepsilon}(\omega, \mathbf{k})$, of a local material is necessarily a quadratic function of the wave vector $\mathbf{k}$. This suggests that the local parameters are related to the first- and second-order derivatives of $\underline{\varepsilon}(\omega, \mathbf{k})$ with respect to $\mathbf{k}$. This topic is further developed in Sections 10.6.2 and 10.6.3.

The importance of the local effective parameters can be appreciated only in problems that involve interfaces between different materials. Only the local effective parameters can be used to solve boundary value problems using the classical boundary conditions (continuity of the tangential components of the macroscopic electric and magnetic fields) at an interface [39]. The reason is clear: while the local model (Equation 10.6) is valid in the spatial domain, the nonlocal model (Equation 10.11) is valid only in the Fourier domain, i.e., for unbounded homogeneous materials. The solution of boundary value problems involving spatially dispersive materials is difficult and involves the use of completely different concepts and methods [4,39]. We return to this topic in Section 10.7.

## 10.6.2 Spatial Dispersion Effects of First and Second Order

Equation 10.68 implies that in a local material the dyadics $\underline{\boldsymbol{\xi}}$ and $\underline{\boldsymbol{\zeta}}$ that characterize bianisotropic effects can be calculated from the first-order derivatives of the dielectric function, $\underline{\varepsilon}(\omega, \mathbf{k})$, with respect to $\mathbf{k}$, and that the magnetic permeability is completely determined by the second-order derivatives of the dielectric function. These properties suggest that it may be possible to extract the local effective parameters of a generic composite material by expanding the dielectric function in a Taylor series [31]:

$$\underline{\boldsymbol{\varepsilon}}(\omega, \mathbf{k}) \approx \underline{\boldsymbol{\varepsilon}}(\omega, \mathbf{0}) + \sum_n \frac{\partial \underline{\boldsymbol{\varepsilon}}}{\partial k_n}(\omega, \mathbf{0}) k_n + \frac{1}{2} \sum_{n,m} \frac{\partial^2 \underline{\boldsymbol{\varepsilon}}}{\partial k_n \partial k_m}(\omega, \mathbf{0}) k_n k_m \tag{10.69}$$

This expansion is meaningful only in the case of weak spatial dispersion. Otherwise, the Taylor expansion is not accurate and local parameters cannot be defined. In the above, the indices of summation are such that $m, n = x, y, z$.

Comparing Equations 10.68 and 10.69, it is evident that the local parameters must verify

$$\underline{\varepsilon}_r - \underline{\boldsymbol{\xi}} \cdot \underline{\boldsymbol{\mu}}_r^{-1} \cdot \underline{\boldsymbol{\zeta}} = \frac{\underline{\boldsymbol{\varepsilon}}}{\varepsilon_0}(\omega, \mathbf{0}) \tag{10.70}$$

On the other hand, from the symmetry property, $\underline{\varepsilon}(\omega, \mathbf{k}) = \underline{\varepsilon}^{t}(\omega, -\mathbf{k})$, enunciated in Section 10.3.5, it is clear that the first-order derivatives, $\frac{\partial \underline{\varepsilon}}{\partial k_n}(\omega, \mathbf{0})$, are antisymmetric dyadics, whereas the second-order derivatives, $\frac{\partial^2 \underline{\varepsilon}}{\partial k_n \partial k_m}(\omega, \mathbf{0})$, are symmetric dyadics. This implies that the first-order derivatives can be completely specified by 9 independent parameters, whereas the second-order derivatives can be completely specified by 36 independent parameters.

The dyadics $\underline{\boldsymbol{\xi}}$ and $\underline{\boldsymbol{\zeta}}$ are chosen so that they satisfy the symmetry relation [33]*

$$\underline{\boldsymbol{\xi}} = -\underline{\boldsymbol{\zeta}}^{t} \tag{10.71}$$

Imposing that the second terms on the right-hand side of Equations 10.68 and 10.69 are coincident, it may be proven that $\underline{\boldsymbol{\zeta}}$ must be such that

$$\underline{\boldsymbol{\zeta}} = \underline{\boldsymbol{\mu}}_{r} \cdot \frac{\omega}{c} \sum_{n} \left( j\mathbf{q}_n \hat{\mathbf{u}}_n - \frac{1}{2} j\mathbf{q}_n \cdot \hat{\mathbf{u}}_n \underline{\mathbf{I}} \right)$$

$$j\mathbf{q}_n = \frac{1}{2} \sum_{m} \frac{1}{\varepsilon_0} \hat{\mathbf{u}}_m \cdot \frac{\partial \underline{\boldsymbol{\varepsilon}}}{\partial k_n}(\omega, \mathbf{0}) \times \hat{\mathbf{u}}_m \tag{10.72}$$

where $\hat{\mathbf{u}}_n$ is a generic unit vector directed along a coordinate axis. Thus, once the magnetic permeability $\underline{\boldsymbol{\mu}}_{r}$ is determined, the remaining local parameters can be easily obtained using Equations 10.70 through 10.72.

To calculate $\underline{\boldsymbol{\mu}}_{r}$, it is necessary to impose that the third terms on the right-hand side of Equations 10.68 and 10.69 are equal for arbitrary $\mathbf{k}$. However, it is simple to verify that, in general, there is no solution for $\underline{\boldsymbol{\mu}}_{r}$ that ensures such a condition. This is a consequence of the second-order derivatives of the dielectric function being characterized by 36 independent parameters. From a physical point of view, it is possible to understand this limitation by noting that spatial dispersion of the second order (third term in the right-hand side of Equation 10.69) emerges not only due to the eddy currents associated with magnetic dipole moments, but also due to the quadrupole moment density [31]. We remind that in Equation 10.68 the effects of the quadrupole density were neglected. Despite the described difficulties, in some circumstances it may be possible to use symmetry arguments to directly extract $\underline{\boldsymbol{\mu}}_{r}$ from the second-order derivatives of the dielectric function. This is illustrated in the next section.

To illustrate the application of the described theory and the calculation of the dyadics $\underline{\boldsymbol{\xi}}$ and $\underline{\boldsymbol{\zeta}}$ in a material with strong magnetoelectric coupling, we consider next a medium formed by an array of infinitely long metallic helices [38] oriented along the $z$-direction, as illustrated in Figure 10.3. We restrict our attention to the case of propagation in the *xoy*-plane. Only in such conditions the effects of spatial dispersion can be considered weak, and local parameters can be defined. In reference [38], the local parameters were extracted directly from the nonlocal dielectric function using ideas analogous to those developed here. It was verified that to a good approximation, the local parameters are such that $\underline{\varepsilon}_{r} = \varepsilon_t(\hat{\mathbf{u}}_x\hat{\mathbf{u}}_x + \hat{\mathbf{u}}_y\hat{\mathbf{u}}_y) + \varepsilon_{zz}\hat{\mathbf{u}}_z\hat{\mathbf{u}}_z$, $\underline{\boldsymbol{\zeta}} = \zeta_{zz}\hat{\mathbf{u}}_z\hat{\mathbf{u}}_z = -\underline{\boldsymbol{\xi}}^{t}$, and $\underline{\boldsymbol{\mu}}_{r} = \hat{\mathbf{u}}_x\hat{\mathbf{u}}_x + \hat{\mathbf{u}}_y\hat{\mathbf{u}}_y + \mu_{zz}\hat{\mathbf{u}}_z\hat{\mathbf{u}}_z$. In Figure 10.4 the extracted effective parameters are plotted as a function frequency for a material with radius of the helices $R = 0.4a$, radius of the wires $r_w = 0.01a$, and helix pitch $a_z = 0.5a$. It is seen that the effective permeability is less than one, and is approximately independent of frequency. Likewise, the transverse effective permittivity (not shown in the figure) is $\varepsilon_t \approx 1.77$, and is also nearly independent of frequency. On the other hand, since the helical wires are assumed infinitely long, the effective permittivity along $z$ exhibits a plasmonic behavior being negative below a certain plasma frequency.

*This is possible because the first-order derivatives of the dielectric function can be characterized using only nine independent parameters.

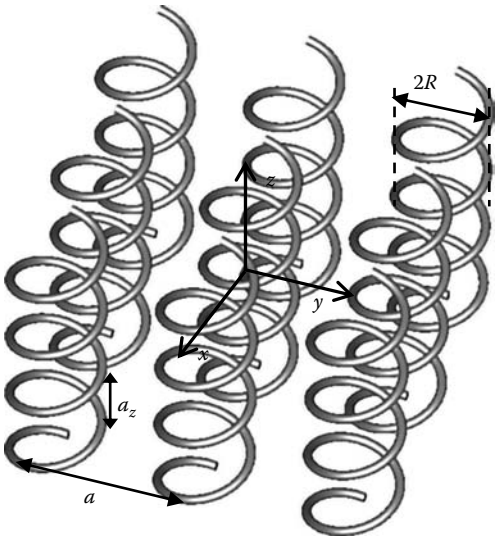


**FIGURE 10.3** Geometry of a periodic array of infinitely long PEC helices arranged in a square lattice. (Reprinted from Silveirinha, M.G., *IEEE Trans. Antennas Propagat.*, 56, 390, 2008. With permission.)

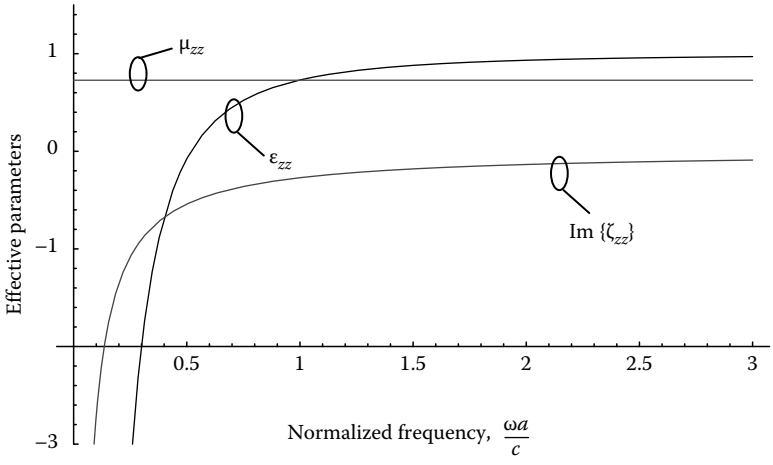


**FIGURE 10.4** Effective parameters ($xoy$-plane propagation) for a material with $R = 0.4a$, $r_w = 0.01a$, and $a_z = 0.5a$. (Reprinted from Silveirinha, M.G., *IEEE Trans. Antennas Propagat.*, 56, 390, 2008. With permission.)

Interestingly, the chirality parameter Im $\{\zeta_{zz}\}$ has a resonant behavior near the static limit. This is a very unusual property, since in general the magnetoelectric coupling is negligible in the quasistatic limit. This property can be understood by noting that the length of the helical wires is infinite, and thus the chiral effects can be greatly enhanced at low frequencies. This anomalous phenomenon is also consistent with the analysis of [40] based on a local field approach. The strong magnetoelectric coupling characteristic of this microstructured material may be exploited to design a very efficient and thin polarization transformer; which converts a linearly polarized wave into a circularly polarized wave [38].

### 10.6.3 Characterization of Materials with Negative Parameters

In what follows, the formalism developed in the previous sections is applied to characterize the local parameters of complex structures formed by split-ring resonators and metallic wires. It is well known that such microstructured materials may have simultaneously negative permittivity and permeability in a certain frequency range [6].

As discussed in Section 10.6.2, the local parameters can be obtained by expanding the dielectric function $\underline{\varepsilon}(\boldsymbol{\omega}, \mathbf{k})$ in powers of the wave vector. In the examples considered here, the inclusions and the lattice have enough symmetries so that the effective medium is nongyrotropic, i.e., the first-order derivatives of $\underline{\varepsilon}(\omega, \mathbf{k})$ with respect to $\mathbf{k}$ vanish at the origin, or equivalently (see Equation 10.72), the magnetoelectric tensors $\underline{\boldsymbol{\xi}}$ and $\underline{\boldsymbol{\zeta}}$ are identically zero. This can be ensured by using a magnetic particle formed by two parallel rings with splits: the broadside coupled split-ring resonator (BC-SRR). As proven in [41], such a magnetic particle does not permit bianisotropic effects.

It is assumed here that the metallic wires are oriented along the $y$-direction, and that the BC-SRRs are parallel to the $xoy$ plane (see the inset of Figure 10.6). Due to symmetry, this implies that the magnetic permeability of the artificial medium is of the form $\underline{\boldsymbol{\mu}_\mathbf{r}}(\omega) = \hat{\mathbf{u}}_x\hat{\mathbf{u}}_x + \hat{\mathbf{u}}_y\hat{\mathbf{u}}_y + \mu_{zz}\hat{\mathbf{u}}_z\hat{\mathbf{u}}_z$. Since the magnetoelectric tensors must vanish, Equation 10.70 demonstrates that the local permittivity is given by

$$\underline{\varepsilon_\mathrm{r}}(\omega) = \frac{\underline{\boldsymbol{\varepsilon}}}{\varepsilon_0}(\omega, \mathbf{0}) \tag{10.73}$$

On the other hand, substituting the formula for magnetic permeability into Equation 10.68, it is simple to verify that to obtain an identity it is necessary that

$$\mu_{zz}(\omega) = \frac{1}{1 - \left(\frac{\omega}{c}\right)^2 \frac{1}{2\varepsilon_0} \left.\frac{\partial^2 \varepsilon_{yy}}{\partial k_x^2}\right|_{\mathbf{k}=0}} \tag{10.74}$$

where $\varepsilon_{yy} = \hat{\mathbf{u}}_y \cdot \underline{\varepsilon} \cdot \hat{\mathbf{u}}_y$. Hence, provided the considered metamaterial can be characterized using a local homogenization model, its constitutive parameters are necessarily given by Equations 10.73 and 10.74. Consistently, with the discussion of Section 10.6.2, the magnetic permeability is a function of the second-order derivatives of the dielectric function with respect to the wave vector.

In the example considered here, it is assumed that the lattice spacings along the coordinate axes are $a_x = a_y \equiv a$, and $a_z = 0.5a$ (the lattice is tetragonal). The BC-SRRs have a mean radius, $R_\mathrm{med} = 0.4a$, and an angular split of 10°. To simplify the numerical implementation of the homogenization method, it was considered that the rings are formed by thin metallic wires with a circular cross section, and a radius, $0.01a$. The distance between the two rings (relative to the mid-plane of each ring) is $d = 0.125a$. The continuous metallic wires also have a radius, $0.01a$.

Using the Equations 10.58, 10.73, and 10.74, the local effective parameters $\underline{\boldsymbol{\varepsilon}_\mathbf{r}}(\boldsymbol{\omega})$ and $\mu_{zz}(\omega)$ were computed as a function of frequency. The numerical results were obtained using five expansion functions $\mathbf{w}_n = \mathbf{w}_{n,\mathbf{k}}(\mathbf{r})$ per wire/ring. The derivatives with respect to $\mathbf{k}$ in Equation 10.74 were evaluated using numerical methods. The extracted effective permittivity $\varepsilon_{yy}$ and effective permeability $\mu_{zz}$ are depicted in Figure 10.5 for three configurations of the metamaterial. The permittivity along $z$, $\varepsilon_{zz} = 1$, is not shown in the figure. Consistently with the results of [6], the extracted parameters predict that there is a frequency window, $0.86 < \omega a/c < 1.04$, where the effective permittivity and permeability are simultaneously negative (curve $(a)$). If the continuous wires are removed and the metamaterial is formed by only BC-SRRs (curve $(b)$) the effective permeability is nearly unchanged, while the effective permittivity becomes positive in the indicated frequency range. If the BC-SRRs are removed the permeability becomes unity, while the effective permittivity remains negative, as shown in curve $(c)$.

The extracted local parameters, $\varepsilon_{yy}$ and $\mu_{zz}$, were used to compute the dispersion characteristic $\omega = \omega(k_x)$ of the metamaterial for propagation along the $x$-direction. The corresponding band structure is depicted in Figure 10.6 (solid black lines). In order to confirm these results and check the

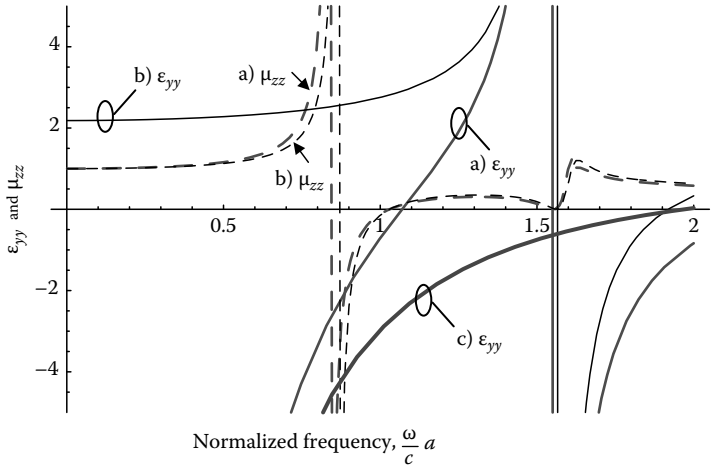


**FIGURE 10.5** Extracted effective permittivity (solid lines) and effective permeability (dashed lines) for a metamaterial formed by (a) continuous wires + BC-SRRs (medium thick light gray lines), (b) only BC-SRRs (thin black lines), and (c) only continuous wires (thick dark gray line). (Reprinted from Silveirinha, M.G., *Phys. Rev. B*, 75, 115104, 2007. With permission.)

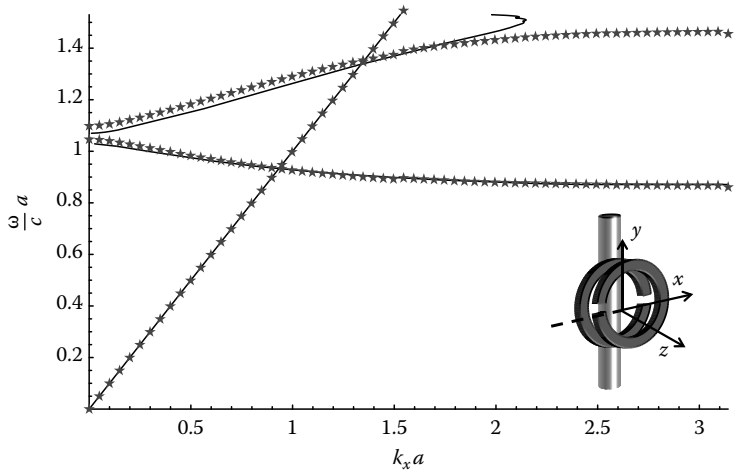


**FIGURE 10.6** Band structure of a composite material formed by wires + BC-SRRs (geometry of the unit cell is shown in the inset). The solid black lines were calculated using the extracted $\varepsilon_{yy}$ and $\mu_{zz}$. The discrete "star" symbols were obtained using the full wave hybrid method introduced in [42]. (Reprinted from Silveirinha, M.G., *Phys. Rev. B*, 75, 115104, 2007. With permission.)

accuracy of the homogenization model, the full wave hybrid method introduced in [42] was used to compute the "exact" band structure of the composite material (star symbols in Figure 10.6). It is seen that the homogenization and full wave results compare very well, especially in the range $\omega a/c < 1.3$. In particular, the frequency band where the material has permittivity and permeability simultaneously negative is predicted with very good accuracy, even for values of $k_x$ near the edge of the Brillouin zone. For frequencies above $\omega a/c = 1.4$, near the resonance of $\varepsilon_{yy}$, the agreement quickly deteriorates

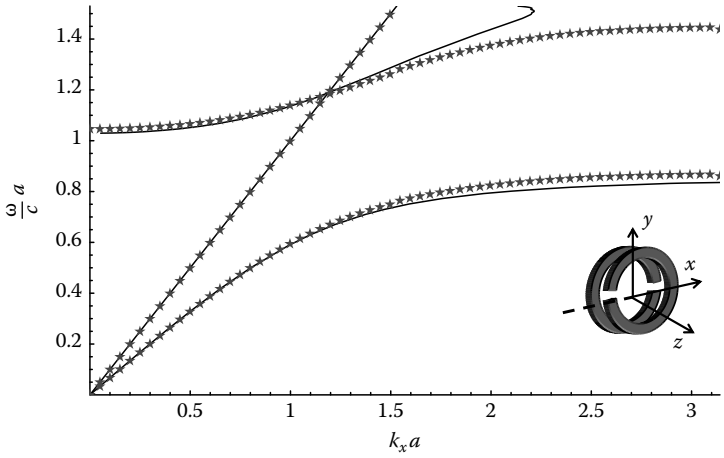


**FIGURE 10.7** Band structure of a composite material formed by BC-SRRs (geometry of the unit cell is shown in the inset). The legend is as in Figure 10.6. (Reprinted from Silveirinha, M.G., *Phys. Rev. B*, 75, 115104, 2007. With permission.)

and the magnetic permeability ceases to have meaning. This can be explained by noting that $\varepsilon_{yy}$ varies fast near the resonance, and thus, the Taylor series of the dielectric function with respect to **k** fails to describe accurately the dependence on the wave vector. Thus, spatial dispersion effects cannot be ignored near the resonance.

Similar band structure calculations were made for the case in which the continuous wires are removed, and the material is formed uniquely by BC-SRRs. These results are shown in Figure 10.7, further demonstrating the accuracy of the homogenization model. Consistently, with the results of [6], the frequency region where the composite material has simultaneously negative parameters becomes a frequency band gap when the metallic wires are removed.

## 10.7 The Problem of Additional Boundary Conditions

At a sharp boundary between two different materials the macroscopic fields are, in general, discontinuous due to the sudden change of the material parameters. The classical procedure to characterize the fields near the interface is to provide certain jump conditions to connect the fields on the two sides of the interface, and in this way obtain a unique solution defined in all space. For local materials, the jump conditions correspond to the continuity of the tangential components of the electric and magnetic fields. These boundary conditions are, in general, derived by considering a transition layer of infinitesimal thickness, and by using an integral formulation of Maxwell's equations [12]. Alternatively, for dielectric crystals, the classical boundary conditions can also be derived directly from the expansion of the microscopic fields into Floquet modes using the concept of transverse averaged fields [43]. The direct application of the classical boundary conditions to structured materials may not yield satisfactory results when the wavelength of the radiation is only moderately larger than the characteristic dimensions of the unit cell, say 10 times or less [44]. In these conditions, it may not be possible to regard the material as continuous, characterized by the bulk effective parameters, since its intrinsic granularity may not be neglected [43]. The discussion of strategies to overcome these difficulties is out of the scope of this chapter and can be read in [43,44].

In spatially dispersive materials the situation is even more problematic. Even the solution of a simple plane wave scattering problem may not be a trivial task when spatially dispersive materials are involved. The nonlocal character of the material response may cause the emergence of new waves, as

compared to the ordinary case in which only two plane waves can propagate along a fixed direction of space [4]. This implies that the classical boundary conditions are insufficient to relate the fields on the two sides of an interface between a spatially dispersive material and another material. In order that the problem has a unique solution it is necessary to specify also boundary conditions for the internal variables that describe the excitations responsible for the spatial dispersion effects [1]. Or in other words, to remove the extra degrees of freedom it is necessary to consider "additional boundary conditions" (ABCs) [4,5]. The ABC concept has been used in the electromagnetics of spatially dispersive media for many decades [45–48].

The simplest class of ABCs was proposed by Pekar [45], which imposes that either the polarization vector or its spatial derivatives vanish at the interface. Unfortunately, there is no general theory available to derive an ABC for a spatially dispersive material. This is a consequence of the ABCs being dependent on the internal variables of the material. The nature of the ABC depends on the specific microstructure of the material, and can be determined only on the basis of a microscopic model that describes the dynamics of these internal variables.

The objective of this section is to briefly review the theory of ABCs for wire media. This canonical problem is particularly interesting since it can be treated using analytical methods, and perfectly illustrates how ABCs can be derived and employed to characterize the refraction of waves by a spatially dispersive material. Our analysis is based on the theory derived in [43,49,50]. An alternative "ABC-free" motivated approach has been reported in [51].

### 10.7.1 Additional Boundary Conditions for Wire Media

In this section, the refraction and reflection of waves by a wire medium slab are investigated. The wire medium consists of an array of long metallic parallel wires arranged in a periodic lattice, as illustrated in Figure 10.8. The wires are oriented along the $z$ direction and embedded in a host medium with permittivity $\varepsilon_h$. As discussed in Section 10.5.3, this material is strongly spatially dispersive, even in the long wavelength limit [20–22]. As a consequence, it supports three different families of electromagnetic modes in the long wavelength limit: transverse electric to $z$ ($TE^z$) modes, transverse

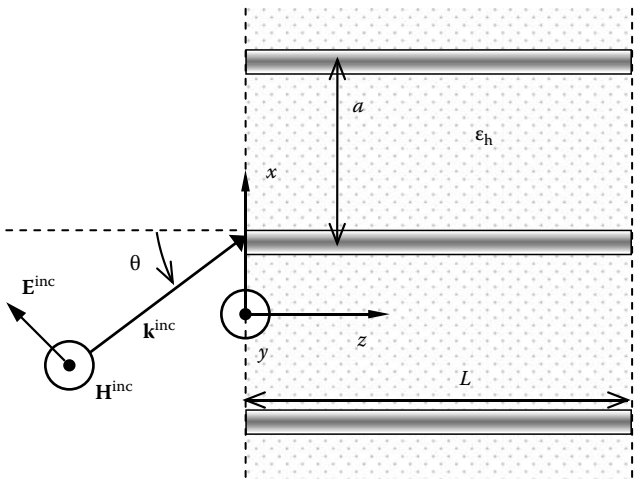


**FIGURE 10.8** A wire medium slab with thickness $L$ is illuminated by a $TM^z$ polarized incoming plane wave. The metallic wires are arranged in a square lattice with lattice constant $a$, and embedded in a dielectric material with permittivity $\varepsilon_h$. (Reprinted from Silveirinha, M.G., Belov, P.A., and Simovski, C.R., *Phys. Rev. B*, 75, 035108, 2007. With permission.)

magnetic to $z$ ($TM^z$) modes, and transverse electromagnetic (TEM) modes [20]. The existence of three different electromagnetic modes implies that the usual boundary conditions (continuity of the tangential component of the electric and magnetic fields) at an interface between the (homogenized) wire medium and another material are not sufficient to solve unambiguously a scattering problem. It can be easily verified that the associated linear system has one degree of freedom [49], and thus the need for an ABC is evident.

In order to derive the ABC, it is necessary to identify some property of the structure under study that can be used to obtain some nontrivial relation between the macroscopic/electromagnetic fields. In the case of the wire medium it is relatively simple to identify such a property. Supposing that the wire medium is adjacent to a nonconductive material (e.g., air) and that the metallic wires are thin, it is evident that the density of the electric surface current at the wires' surface must vanish at the interface:

$$\mathbf{J}_c = 0 \text{ (at the interface)} \tag{10.75}$$

It was proven in [49] that this property implies that the macroscopic electric field satisfies the following ABC at an interface with air*:

$$\varepsilon_h \, \mathbf{E} \cdot \hat{\mathbf{u}}_z \big|_{\text{wire medium side}} = \mathbf{E} \cdot \hat{\mathbf{u}}_z \big|_{\text{air side}} \tag{10.76}$$

It is important to note that the above condition is not equivalent to the continuity of the electric displacement vector, since the effective permittivity of the wire medium is not $\varepsilon_h$, but is instead given by Equation 10.63. The ABC is also valid in the case of wires with finite conductivity [11], and when the wires are tilted with respect to the interface with air [50].

The ABC (Equation 10.76) together with the classical boundary conditions can be used to characterize the reflection and refraction of waves by slabs of wire media. To illustrate this property and the accuracy of the described theory, in Figure 10.9 the amplitude of the reflection coefficient is plotted as a function of the normalized frequency for plane wave incidence along $\theta = 45°$. The solid lines correspond to full wave results obtained using the MoM, and the dashed lines represent the results obtained using the homogenization model and the ABC (Equation 10.76). The lattice constant is $a$, the radius of the wires is $r_w = 0.01a$, and the wires are embedded in air, $\varepsilon_h = 1$. It is seen that the agreement between the homogenization model and the full wave results is excellent, for both thin and thick wire medium slabs, and for normalized frequencies as large as $\omega a/c = 2.0$. It was proven in [11,52] that the proposed ABC may be used to characterize the imaging properties of wire media slabs upto infrared frequencies.

The ABC (Equation 10.76) is valid provided the material adjacent to the wire medium is nonconductive. However, in several configurations of interest the metallic wires are connected to a ground plane, as illustrated in Figure 10.10. For example, textured and corrugated surfaces have important applications in the design of high-impedance surfaces, impedance boundaries, and suppression of guided modes [29,53,54]. When the metallic wires are connected to a conductive material, it is not true that the density of current $\mathbf{J}_c$ vanishes at the interface, and thus the ABC (Equation 10.76) does not apply.

Even though Equation 10.75 does not hold at an interface of a wire medium connected to a PEC ground plane, it is relatively simple to obtain the boundary condition verified by the microscopic electric current in a such scenario. More specifically, it can be proven that the electric density of surface charge, $\sigma_c$, on the surface of a generic wire satisfies [50]

$$\sigma_c = 0 \text{ (at the interface)} \tag{10.77}$$

*In this section, the macroscopic fields, $\langle \mathbf{E} \rangle$ and $\langle \mathbf{B} \rangle / \mu_0$, are simply denoted by $\mathbf{E}$ and $\mathbf{H}$, respectively, to avoid complicating the notations unnecessarily.

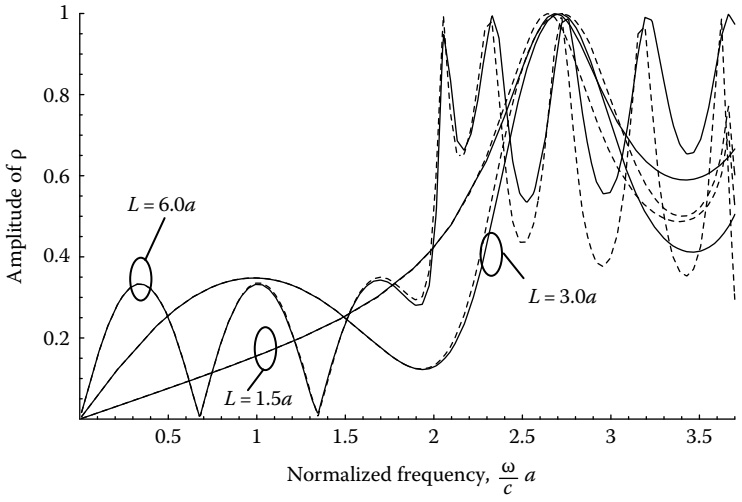


**FIGURE 10.9** Amplitude of the reflection coefficient as a function of the normalized frequency for incidence along θ = 45° and different values of the slab thickness $L$ (solid line: full wave results; dashed line: homogenization model). The wires are embedded in air and have a radius $r_w = 0.01a$. (Reprinted from Silveirinha, M.G., *IEEE Trans. Antennas Propagat.*, 54, 1766, 2006. With permission.)

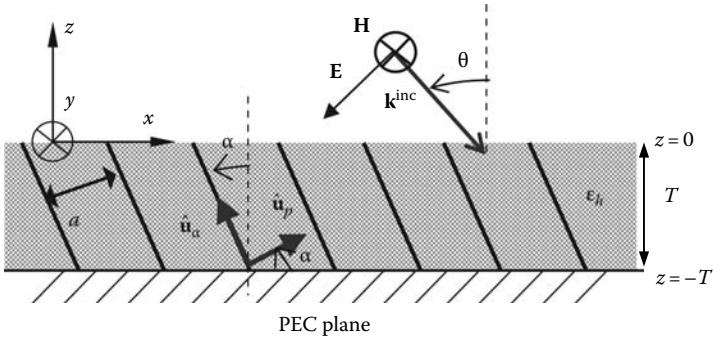


**FIGURE 10.10** A wire medium slab is connected to a ground plane. The metallic wires are arranged in a square lattice with a lattice constant $a$. The wires may be tilted with respect to the interfaces (normal to the $z$-direction) by an angle α. The structure is periodic along the $x$ and $y$ directions. (Reprinted from Silveirinha, M.G., Fernandes, C.A., and Costa, J.R., *New J. Phys.*, 10, 053011(1–17), 2008. With permission.)

A detailed analysis demonstrates that this property, which is intrinsically related to the microstructure of the material, implies that the macroscopic fields verify the following ABC at the PEC interface [50],

$$\left(\mathbf{k}_{||}\cdot\hat{\mathbf{u}}_\alpha+\hat{\mathbf{u}}_z\cdot\hat{\mathbf{u}}_\alpha j\frac{\mathrm{d}}{\mathrm{d}z}\right)\left(\omega\varepsilon_0\varepsilon_h\hat{\mathbf{u}}_\alpha\cdot\mathbf{E}+\hat{\mathbf{u}}_\alpha\times\left(\mathbf{k}_{||}+\hat{\mathbf{u}}_z j\frac{\mathrm{d}}{\mathrm{d}z}\right)\cdot\mathbf{H}\right)=0 \tag{10.78}$$

where

$\hat{\mathbf{u}}_\alpha$ is the unit vector along the direction of the wires (see Figure 10.10)
$\hat{\mathbf{u}}_z$ is the normal to the interface
$\mathbf{k}_{||}$ is the component of the wave vector parallel to the interface

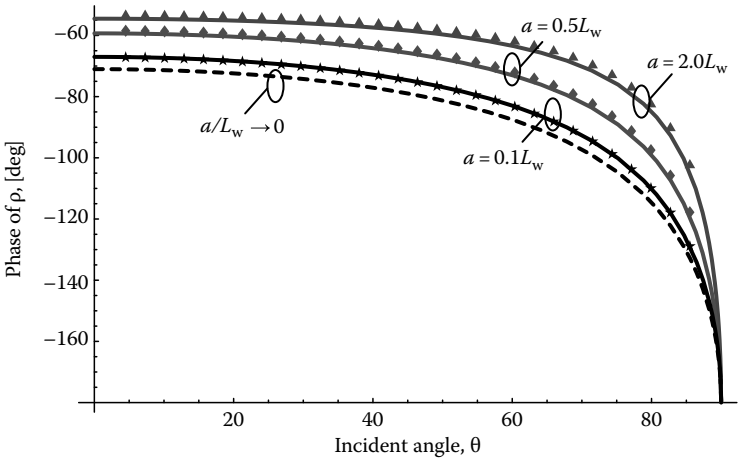


**FIGURE 10.11** Reflection characteristic for a substrate formed by tilted wires ($\alpha = 45°$) connected to a PEC plane. The wires are embedded in a dielectric with $\varepsilon_h = 4.0$ and thickness $T$ such that $T\sqrt{\varepsilon_h}\omega/c = \pi/4$. The spacing between the wires, $a$, associated with each curve is indicated in the figure. The radius of the wires is $r_w = 0.05a$, and the length of the wires is $L_w = T \sec \alpha$. The solid lines were obtained with the homogenization model, and the discrete symbols were obtained using the commercial simulator CST Microwave Studio. (Reprinted from Silveirinha, M.G., Fernandes, C.A., and Costa, J.R., *New J. Phys.*, 10, 053011(1–17), 2008. With permission.)

This ABC together with the classical boundary condition, $\hat{\mathbf{u}}_z \times \mathbf{E} = 0$, completely characterizes the reflection of waves by a wire medium slab connected to a ground plane. As an example of the application of such a result, we consider the geometry of Figure 10.10 where an incoming plane wave is reflected by a grounded wire medium slab. The reflection coefficient may be computed using homogenization methods by matching the fields in the air and wire medium regions at the interface $z = 0$ and using the ABC (Equation 10.76) and the classical boundary conditions, and by enforcing the ABC (Equation 10.78) and $\hat{\mathbf{u}}_z \times \mathbf{E} = 0$ at the interface with the conducting plane at $z = -T$ [50]. The calculated reflection characteristic is depicted in Figure 10.11 (solid lines) for different lattice spacings. The parameters of the microstructured substrate are given in the legend of the figure. The discrete symbols correspond to data obtained using the commercial electromagnetic simulator, CST Microwave Studio. It is seen that homogenization results compare very well with full wave simulations, both when the wires are very densely packed ($a = 0.1L_w$) and when the wires are loosely packed ($a = 2.0L_w$), where $L_w = T \sec\alpha$ is the length of the metallic wires. It can be verified that in the limit in which $a/L_w \to 0$, the wire medium behaves as a material with extreme optical properties, and the interface $z = 0$ may be characterized by an impedance boundary condition [50]. Arrays of tilted metallic wires connected to a ground plane have great potentials in the realization of high-impedance substrates.

Even though the results presented in this chapter deal exclusively with arrays of parallel wires, the described ABCs can also be applied to other more complex topologies of wire media [23,43].

## References

1. J. van Kranendonk and J. E. Sipe, Foundations of the macroscopic electromagnetic theory of dielectric media, chapter 5 in *Progress in Optics XV*, (ed. by E. Wolf), New York: North-Holland, 1977.
2. G. Russakov, A derivation of the macroscopic Maxwell equations, *Am. J. Phys*, 38, 1188, 1970.

3. J. Sipe and J. V. Kranendonk, Macroscopic electromagnetic theory of resonant dielectrics *Phys. Rev. A*, 9, 1806, 1974.
4. V. Agranovich and V. Ginzburg, *Spatial Dispersion in Crystal Optics and the Theory of Excitons*, New York: Wiley-Interscience, 1966.
5. G. D. Mahan and G. Obermair, Polaritons at surfaces, *Phys. Rev*., 183, 834, 1969.
6. D. R. Smith, Willie, J. Padilla, D. C. Vier, S. C. Nemat-Nasser, and S. Schultz, A Composite medium with simultaneously negative permeability and permittivity, *Phys. Rev. Lett*., 84, 4184, 2000.
7. M. Silveirinha and N. Engheta, Tunneling of electromagnetic energy through sub-wavelength channels and bends using near-zero-epsilon materials, *Phys. Rev. Lett*., 97, 157403, 2006.
8. J. B. Pendry, Negative refraction makes a perfect lens, *Phys. Rev. Lett*., 85, 3966, 2000.
9. C. Luo, S. G. Johnson, J. D. Joannopoulos, and J. B. Pendry, Subwavelength imaging in photonic crystals, *Phys. Rev. B*, 68, 045115, 2003.
10. P. A. Belov, Y. Hao, and S. Sudhakaran, Subwavelength microwave imaging using an array of parallel conducting wires as a lens, *Phys. Rev. B*, 73, 033108, 2006.
11. M. G. Silveirinha, P. A. Belov, and C. R. Simovski, Subwavelength imaging at infrared frequencies using an array of metallic nanorods, *Phys. Rev. B*, 75, 035108, 2007.
12. J. D. Jackson, *Classical Electrodynamics*, Sect. 6.6, New York: Wiley, 1998.
13. S. Datta, C. T. Chan, K. M. Ho, and C. M. Soukoulis, Effective dielectric constant of periodic composite structures, *Phys. Rev. B*, 48, 14936, 1993.
14. W. Lamb, D. M. Wood, and N. W. Ashcroft, Long-wavelength electromagnetic propagation in heterogeneous media, *Phys. Rev. B*, 21, 2248, 1980.
15. M. G. Silveirinha and C. A. Fernandes, Effective permittivity of metallic crystals: A periodic Green's function formulation, *Electromagnetics*, 8, 647, 2003.
16. O. Ouchetto, C.-W. Qiu, S. Zouhdi, L.-W. Li, and A. Razek, Homogenization of 3-D periodic bianisotropic metamaterials, *IEEE Trans. Microwave Theory Technol*., 54, 3893, 2006.
17. D. R. Smith and J. B. Pendry, Homogenization of metamaterials by field averaging, *J. Opt. Soc. Am. B*, 23, 391, 2006.
18. D. R. Smith, S. Schultz, P. Markos, and C. M. Soukoulis, Determination of effective permittivity and permeability of metamaterials from reflection and transmission coefficients, *Phys. Rev. B*, 65, 195104, 2002.
19. C. R. Simovski, Bloch material parameters of magneto-dielectric metamaterials and the concept of Bloch lattices, *Metamaterials*, 1, 62, 2007.
20. P. A. Belov, R. Marqués, S. I. Maslovski, I. S. Nefedov, M. Silveirinha, C. R. Simovski, and S. A. Tretyakov, Strong spatial dispersion in wire media in the very large wavelength limit, *Phys. Rev. B*, 67, 113103, 2003.
21. M. G. Silveirinha, Nonlocal homogenization model for a periodic array of epsilon-negative rods, *Phys. Rev. E*, 73, 046612, 2006.
22. A. L. Pokrovsky and A. L. Efros, Nonlocal electrodynamics of two-dimensional wire mesh photonic crystals, *Phys. Rev. B*, 65, 045110, 2002.
23. M. G. Silveirinha and C. A. Fernandes, Homogenization of 3D-connected and non-connected wire metamaterials, *IEEE Trans. Microwave Theory Technol*., 53, 1418, 2005.
24. P. A. Belov and C. R. Simovski, Homogenization of electromagnetic crystals formed by uniaxial resonant scatterers, *Phys. Rev. E*, 72, 026615, 2005.
25. M. G. Silveirinha and P. A. Belov, Spatial dispersion in lattices of split ring resonators with permeability near zero, *Phys. Rev. B(BR)*, 77, 233104, 2008.
26. D. Sjoberg, Dispersive effective material parameters, *Microwave Opt. Technol. Lett*., 48, 2629, 2006.
27. J. Li and J. B. Pendry, Non-local effective medium of metamaterial, arxiv:cond-mat/0701332v1, 2007.

28. J. D. Baena, L. Jelinek, R. Marqués, and M. G. Silveirinha, Unified homogenization theory for magnetoinductive and electromagnetic waves in split-ring-metamaterials, *Phys. Rev. A*, 78, 013842, 2008.
29. M. G. Silveirinha, C. A. Fernandes, and J. R. Costa, Electromagnetic characterization of textured surfaces formed by metallic pins, *IEEE Trans. Antennas Propagat*., 56, 405, 2008.
30. M. G. Silveirinha, A metamaterial homogenization approach with application to the characterization of microstructured composites with negative parameters, *Phys. Rev. B*, 75, 115104, 2007.
31. L. D. Landau and E. M. Lifshitz, *Electrodynamics of Continuous Media*, Course of Theoretical Physics, vol. 8, Oxford: Elsevier Butterworth-Heinemann, 2004.
32. I. V. Lindell, A. H. Sihvola, S. A. Tretyakov, and A. Viitanen, *Electromagnetic Waves in Chiral and Bi-Isotropic Media*, Boston, MA: Artech House, 1994.
33. A. N. Serdyukov, I. V. Semchenko, S. A. Tretyakov, and A. Sihvola, *Electromagnetics of Bi-Anisotropic Materials: Theory and Applications*, Amsterdam, the Netherlands: Gordon and Breach Science Publishers, 2001.
34. M. G. Silveirinha, Generalized Lorentz-Lorenz formulas for microstructured materials, *Phys. Rev. B*, 76, 245117, 2007.
35. M. G. Silveirinha and C. A. Fernandes, A new acceleration technique with exponential convergence rate to evaluate the periodic green function, *IEEE Trans. Antennas Propagat*., 53, 347, 2005.
36. P. P. Ewald, Die Berechnung optischer und elektrostatistischer Gitterpotentiale, *Ann. Der Physik*, 64, 253, 1921.
37. R. E. Collin, *Field Theory of Guided Waves*, 2nd edn., New York: IEEE Press, 1991.
38. M. G. Silveirinha, Design of linear-to-circular polarization transformers made of long densely packed metallic helices *IEEE Trans. Antennas Propagat*., 56, 390, 2008.
39. A. P. Vinogradov and I. I. Skidanov, On the problem of constitutive parameters of composite materials, *Proceedings of the Bianisotropics 2000*, Lisbon, Portugal, pp. 17–22, 2000.
40. P. A. Belov, C. R. Simovski and S.A. Tretyakov, Example of bianisotropic electromagnetic crystals: The spiral medium, *Phys. Rev. E*, 67, 056622, 2003.
41. R. Marqués, F. Medina, and R. Rafii-El-Idrissi, Role of bianisotropy in negative permeability and left-handed metamaterials, *Phys. Rev. B*, 65, 144440, 2002.
42. M. G. Silveirinha and C. A. Fernandes, A hybrid method for the efficient calculation of the band structure of 3D metallic crystals, *IEEE Trans. Microwave Theory Technol*., 52, 889, 2004.
43. M. G. Silveirinha and C. A. Fernandes, Transverse average field approach for the characterization of thin metamaterial slabs, *Phys. Rev. E*, 75, 036613, 2007.
44. C. R. Simovski and S. A. Tretyakov, Local constitutive parameters of metamaterials from an effective-medium perspective, *Phys. Rev. B*, 75, 195111, 2007.
45. S. I. Pekar, Theory of the electromagnetic waves in crystals with excitons, *Sov. Phys. JETP*, 6, 785, 1958.
46. A. R. Melnyk, M. J. Harrison, Theory of optical excitation of plasmons in metals, *Phys. Rev. B*, 2, 835, 1970.
47. W. A. Davis and C. M. Krowne, The effects of drift and diffusion in semiconductors on plane wave interaction at interfaces, *IEEE Trans. Antennas Propagat*., 36, 97, 1998.
48. K. Henneberger, Additional boundary conditions: An historical mistake, *Phys. Rev. Lett*., 80, 2889, 1998.
49. M. G. Silveirinha, Additional boundary condition for the wire medium, *IEEE Trans. Antennas Propagat*., 54, 1766, 2006.
50. M. G. Silveirinha, C. A. Fernandes, and J. R. Costa, Additional boundary condition for a wire medium connected to a metallic surface, *New J. Phys*., 10, 053011(1–17), 2008.
51. I. S. Nefedov, A. J. Viitanen, and S. A. Tretyakov, Electromagnetic wave refraction at an interface of a double wire medium *Phys. Rev. B*, 72, 245113, 2005.
52. P. A. Belov and M. G. Silveirinha, Resolution of sub-wavelength transmission devices formed by a wire medium, *Phys. Rev. E*, 73, 056607, 2006.

53. D. Sievenpiper, L. Zhang, R. Broas, N. Alexopolous, and E. Yablonovitch, High-impedance electromagnetic surfaces with a forbidden frequency band, *IEEE Trans. Microwave Theory Technol.*, 47, 2059, 1999.
54. R. J. King, D. V. Thiel, and K. S. Park, The synthesis of surface reactances using an artificial dielectric, *IEEE Trans. Antennas Propagat.*, 31, 471, 1983.